Recent advances on graphene quantum dots : from chemistry and physics to applications

Yan, Yibo; Gong, Jun; Chen, Jie; Zeng, Zhiping; Huang, Wei; Pu, Kanyi; Liu, Jiyang; Chen, Peng

2019

Yan, Y., Gong, J., Chen, J., Zeng, Z., Huang, W., Pu, K., . . . Chen, P. (2019). Recent advances on graphene quantum dots : from chemistry and physics to applications. Advanced Materials, 31(21), 1808283-. doi:10.1002/adma.201808283

https://hdl.handle.net/10356/142854

https://doi.org/10.1002/adma.201808283

WILEY-VCH

ADVANCED MATERIALS

DOI: 10.1002/ ((please add manuscript number))
Article type: Review

Recent Advances on Graphene Quantum Dots: From Chemistry and Physics to Applications

Yibo Yan[1,3], Jun Gong[3], Jie Chen[3], Zhiping Zeng[3], Wei Huang[1], Kanyi Pu[3], Jiyang Liu[2] Peng Chen[3]*

[1]Shaanxi Institute of Flexible Electronics, Northwestern Polytechnical University, 127 West Youyi Road, Xi'an, China
[2]Department of Chemistry, School of Sciences, Zhejiang Sci-Tech University, 928 Second Avenue, Xiasha Higher Education Zone, Hangzhou, China
[3]School of Chemical and Biomedical Engineering, Nanyang Technological University, 70 Nanyang Drive, 637457, Singapore.
E-mail: ChenPeng@ntu.edu.sg

Keywords: graphene quantum dots, zero-dimensional nanomaterials, energy conversion and storage, catalysis, flexible devices, biomedical application

Abstract

Graphene quantum dots (GQDs) which are flat zero-dimensional nanomaerials, have attracted increasing interest because of their exceptional chemicophysical properties and novel applications in energy conversion and storage, electro-/photo-/chemical catalysis, flexible devices, sensing, display, imaging, and theranostics. In this article, we summarize the significant advances in the recent years with comparative and balanced discussion. We emphasize the difference between GQDs and other nanomaterials including their nanocarbon cousins, and highlight the unique advantages of GQDs for specific applications. The current challenges and outlook of this growing field are also discussed.

1. Introduction

Graphene quantum dot (GQD) is the latest addition to the nanocarbon materials family. It is a zero-dimensional (0D) graphene material, characterized by an atomically thin

graphitic plane (typically 1 or 2 layers, <2 nm thick) with lateral dimensions typically <10 nm. Comparing to its 2D counterpart - graphene sheet, GQD offers some unique merits thus new application opportunities, such as, bandgap opening due to quantum confinement, excellent dispersibility, more abundant active sites (edges, functional groups, dopants, etc.), better tunability in chemicophysical properties, and comparable size to biomolecules.[1-3]

Some may regard GQD merely as a giant polyaromatic molecule. But comparing to polycyclic aromatic molecules (e.g., pyrene), GQD has distinct and much more intriguing properties (e.g., much narrower and complex bandgap structure, catalytic abilities) because it is much larger and carries abundant various functional moieties. In the literature, GQD and another kind of 0D carbon materials (carbon dot) are often not carefully distinguished. Here we would like to stress that GQDs and carbon dots (CDs) differ in morphology and properties. CDs are spherical carbon particles. Some are completely amorphous sp^3 carbon while some have a crystalline sp^2 core encapsulated by an amorphous shell. Typically, the diameter of a CD is >3 nm, and CDs have a relatively wide X-ray diffraction (XRD) peak due to the presence of amorphous carbon. Also, unlike GQDs the completely amorphous CDs do not present crystalline lattice under high-resolution transmission electron microscopy (HRTEM). Furthermore, the electronic bandgap structures of GQDs are largely influenced by quantum confinement effect[4] whereas CDs' bandgap structures are dictated by the surface energy traps. Due to these differences, some methods or applications work well for one but may not work well for

the other. Although GQDs and CDs share some similarities, here we exclusively focus on the former.

0D quantum dots can also be derived from other 2D materials (notably, transition metal dichalcogenides).[1] These 2D materials range from insulators (e.g., h-BN, HfS_2), large bandgap semiconductors (e.g., C_3N_4, MoS_2, WS_2), small bandgap semi-conductors (e.g. black phosphorene), and metal-like conductors (e.g., VSe_2). In comparison to GQDs, QDs derived from these 2D materials have distinct intrinsic electronic structures, thickness, and other properties. Some of them can fluoresce in the visible light range for biomedical imaging (e.g., MoS_2 QD), but they are not very stable and dispersible in aqueous solution, not easily to be functionalized, or has very low photoluminescence quantum yield.

Pristine GQD is rarely useful other than for electronic devices. And it cannot be easily synthesized and dispersed. In fact, it is chemical groups, functionalized groups, defects, dopants and their co-existence that make GQDs interesting and versatile. But one may argue that the conductivity (an intrinsic merit of graphene) is lost due to these factors. This is indeed the case and some papers mistakenly claim that their device or electrode performance is benefited from the good conductivity of GQDs. Although the conductivity (laterally through the basal plane) is compromised, many studies have shown that GQDs are able to facilitate charge transfer and transport which occur at the interfaces with electrolytes, reactants or other nanomaterials and are mediated by local active moieties or sp^2 carbon domains.[5, 6]

There are already a number of excellent review articles on graphene quantum dots.[2, 3, 7] For example, we have provided a comprehensive review on the biological applications of GQDs in 2015.[2] Since then, some new exciting developments have been demonstrated, including imaging dynamic cellular processes, in vivo imaging, new design schemes for sensitive fluorescence-based detection, and therapeutic applications. There are also new dimensions have been added to energy and catalysis applications, including novel GQD-based heterojunctions, GQDs as quasi-homogeneous catalysis for chemical conversion, GQDs with intramolecular Z-scheme for photocatalysis. As the field is rapidly evolving, periodic update is necessary. Here we emphasize on the latest significant developments on synthesis, property control, and unique applications in energy conversion and storage, catalysis, flexible devices, and biotechnology (**Figure 1**). We endeavour to offer comparative and balanced views, as well as insights on why GQDs are particularly advantageous for specific applications. Lastly, the current challenges and outlook of this area is provided.

2. Synthesis

The synthetic strategies of GQDs are based on either cutting the larger graphitized carbon materials (top-down) or fusion of small precursor molecules (bottom-up). The top-down methods involve oxidative cutting,[8] reductive cutting,[9] physical grinding,[10] or combination of grinding and cutting.[11] The first bottom-up synthesis of GQDs was reported by Müllen group, based on the stepwise organic synthesis of dendritic polyphenylenes (DPPs) followed by dehydrogenation.[12] Such method can produce

mono-dispersed GQDs with precisely defined molecular structure and size (hence properties). However, it is difficult, tedious, expensive, and of low production yield. And the resulting GQDs prone to π-π stacking because lack of functional groups. We here focus on the bottom-up methods that are realized by fusion of organic molecules under thermal[13] / hydrothermal[14] / solvothermal[15] conditions or carbonization of organic precursors. In comparison, usually top-down methods can utilize cheap bulk carbon materials as precursors and can be applied to any graphitized materials. But they often have relatively low production yield, and require longer reaction time and not-easily-disposable strong oxidants. In general, bottom-up methods offer relatively high yield and the convenience to introduce heteroatom doping during synthesis.

Top-down Methods. Oxidative cleavage is most frequently used for GQD synthesis from larger graphitized carbon materials such as graphite,[8] carbon black,[16, 17] carbon fiber,[18, 19] graphene[20] or graphene oxide (GO).[21-23] Sometimes GQDs derived from GO sheets are called graphene oxide QD[24-27] or reduced graphene oxide QD.[10] To avoid confusion, we simply call them GQDs here.

Strong acids are often used as the oxidants. Among all the precursors, coal is the cheapest. Comparing to graphite (Figure 2a),[8] coal can be more easily cleaved because it contains nano-sized graphitized carbon domains weakly linked by amorphous carbon (Figure 2b).[28] Mixture of highly concentrated nitric and sulfuric acids were used in the original report. But the difficulty to remove sulfuric acid increases the synthesis cost. In principle, nitric acid alone should also work. Carbon black which is a cheap paracrystalline carbon

can also be more easily cleaved by acids comparing to graphite.[17] Using oxidative cleavage, coal and carbon black are more promising than others for large-scale industrial production. Non-acid oxidants (e.g., oxone[29] and H_2O_2[30]), which are free radical initiators, have also been used to exfoliate GQDs (Figure 2c).[31] Comparing to strong acids, these oxidants are less environmentally hazardous. It is noteworthy that oxidatively exfoliated GQDs unavoidably bear abundant oxygenated groups (mainly, -COOH, -OH, C-O-C). The induced oxygenated species and their ratio depend on the used oxidants.

Electrochemical cutting of CVD-grown 3D graphene,[32] carbon nanotube (CNT),[33] graphite,[34] coke[35] and graphene paper[36] can produce uniform-sized GQDs with single layer at high yield. In some experiments where organic solvents are used, their disposal could be an environmental concern. Although 3D graphene gives extremely high efficiency and throughput, it and CNT are expensive precursors. Therefore, electrochemical cutting of graphite is more promising for low-cost and high quality production of GQDs.

Alternative to oxidative cutting, reductive agents (e.g., hydrazine,[9, 37] alkyl amines,[38] ammonia,[39, 40] DMF[41]) cleave oxidized carbon precursors into GQDs by breaking C-O bond in epoxy groups (Figure 2d).[41] Reductive cleavage introduces nitrogen-containing chemical groups and decreases oxygenated groups. The efficiency and the resulting GQD size depend on the abundance of epoxy groups on the precursors. Recently, it has been shown that GO sheets can be reduced and fragmented into GQDs in supercritical water

under hydrothermal condition.[23, 42] This synthesis is completely green and produces GQDs with low amount of oxygenated groups. But the production yield of this method is not reported. Physical cleavage using grinding plus ultrasonication (Figure 2e)[10, 43] or strong shear force in the microfluidizer[44] have also been reported. The thus produced GQDs have low presence of chemical groups and defects.

Bottom-up Methods. It has been demonstrated that methylbenzene and hexabromobenzene can fuse into GQDs free of chemical moieties using Na as the catalyst (Figure 2f).[45] But the synthesis requires extreme caution because Na is super-reactive and methylbenzene is carcinogenic. And undesirably graphene nanoribbon is also simultaneously produced. Citric acid has been used to hydrothermally produce GQDs.[46, 47] Forming intermolecular hydrogen bonds and subsequent dehydration reaction generate sp^2 carbon network (Figure 2g). Note that, when the reaction time is prolonged, CDs instead of GQDs are produced.[48] It has been shown that fusion of norepinephrine molecules (a hormone molecule) under microwave irradiation forms GQDs (Figure 2h).[49] A facile hydrothermal synthesis of OH-bearing GQDs in alkaline solution from 1,3,6-trinitropyrene has also been developed, with high yield and possibility of scale-up production (Figure 2i).[14] It is conceivable that alkaline hydrothermal condition promotes de-nitration and dehydrogenation of 1,3,6-trinitropyrene, and subsequently the resulting dangling carbon bonds covalently link to cause sp^2 fusion between the precursors. In a recent study, salicylic acid was used as the precursor which become aromatic radical under UV irradiation and then fuses into GQDs.[50]

Under high temperature and inert atmosphere, many organic molecules or materials can be carbonized into graphitized materials for subsequent exfoliation of GQDs.[51] An advantage of this strategy is to achieve doping of multiple heteroatoms by readily inheriting from the organic precursors. For example, using a biomolecule ATP as the precursor, a bright N, P co-doped GQD with two-photon-upconversion property is obtained (Figure 2j).[52]

3. Property control

Owing to the small size, the electronic, optical, and catalytic properties of GQDs are highly influenced by various factors including size, functional groups, and dopants. Precisely tailoring these factors are the key to obtain GQDs with well-defined characteristics and therefore ensure their effective uses.

GQD Size. The bandgap of GQD is size-dependent (Figure 3a).[53] GQD size may be controlled by reaction time, temperature (Figure 3b)[54] and reactant concentration (Figure 3c).[38] GQD syntheses, particularly by top-down methods, usually produce GQDs with a wide range of size distribution. Such inhomogeneity leads to excitation-dependent photoluminescence spectrum.[55] The fractionation of GQDs with different sizes can be achieved using ultrafiltration through membranes with defined pore sizes[53] or using gel electrophoresis.[56] Larger size leads to smaller bandgap, hence longer fluorescence emission wavelength.[4]

Oxidization. Creating oxygenated groups on GQDs red-shifts photoluminescence (PL) by introducing intermediate n orbital (Figure 3d),[10] but at the same time compromises PL quantum yield by acting as non-radiative centers.[39, 57] On the contrary, removing the oxygenated groups using reductive agents blue-shifts PL and increases QY, but at the same time sacrifices GQD dispersibility. The abundance of oxygenated group can be controlled by varying oxidative cutting time, strength of the oxidant, or post-synthesis reduction,[10, 58] while the composition of oxygenated species is dictated by the specific oxidants or reductants used for synthesis. Different oxygenated species provide different functionalities. –C=O and –COOH groups on GQD act together as peroxidase mimics,[59] while –COOH and $–SO_3H$ groups can serve as acid catalysts for many reactions.[60, 61]

Heteroatom doping. Doped heteroatoms endow GQDs with altered electronic bandgap structures[62] and catalytic abilities.[63] Heteroatom doping can be realized through post-synthesis processes, for instances, N-doping by heating GQDs under ammonia gas or hydrothermally treating GQDs in ammonia solution.[24-26, 64] N-doping narrows the bandgap (hence widens the light adsorption, as shown in Figure 3e) and prolongs the PL lifetime (because of suppression of charge recombination).[25, 65] Hydrothermal treating GQDs with NaHSe produces orange-fluorescent Se-doped GQDs with a high QY of 29%.[66] But the efficiency of post-synthesis doping is poor.

Doping during the synthesis usually gives higher efficiency. Heteroatom doping can be realized during top-down cutting synthesis via introducing heteroatom source or directly using dopant-containing oxidant or reductant.[67] An N,F and S co-doped GQD has been

prepared by ultrasonicating and microwaving CNTs in ionic liquid 1-methyl-1-propylpiperidiniumbis(trifluoro-methylsulfonyl)imide.[68] Interestingly, doping greatly improved PL quantum yield (QY). Cutting GO by boric acid vapor and ammonia gas in a tube furnace at high temperature produces B,N co-doped GQDs with good catalytic ability for oxygen reduction.[69] Electrochemically cutting graphite in electrolyte with P-containing sodium phytate gives P-doped GQDs.[70] P-doping confers GQD with the good ability to scavenge free radicals. Alternatively, cleaving heteroatom-containing graphitized precursors directly produces doped GQDs. For example, cutting fluorinated graphene by mixed sulfuric and nitric acids under ultrasonication forms F-doped GQDs with up-conversion PL.[71] Cutting polythiophene by NaOH under hydrothermal condition produces S-doped GQDs which are capable of efficient generation of singlet oxygen, deep red emission (680 nm) and strong light absorption.[72] A S-doped GQD has been prepared by hydrothermal treatment of Poly(3-alkylthiophenes) (P3ATs), which exhibits deep red emission up to 700 nm.[73] Moreover, the emission peak of such S-GQDs can be modulated by changing the alkyl chain length of P3ATs.

Heteroatom doping can be readily introduced during bottom-up synthesis using dopant-containing organic precursors or adding dopant source.[74-77, 78-80] Comparing to other doping methods, it is relatively easier to dope on the basal carbon lattice. For example, fusion of N-containing norepinephrine in water under microwave irradiation gives N-doped GQDs, while N,S co-doped GQDs are obtained in S-containing DMSO.[49] Based on fusion of 1,3,6-trinitropyrene precursor, N,S co-doped GQDs are obtained under DMF-based solvothermal condition in the presence of thiourea and NaOH,[15] while S-

doped GQDs are produced under hydrothermal condition in the presence of 3-mercaptopropionic acid.[75]

Based on molecular condensation of citric acid molecules, N-doped GQDs are yielded in the presence of N-containing tris(hydroxymethyl)aminomethane[76] and N,S-doped GQDs are produced in the presence of N,S-containing L-Cysteine.[78] B-doped GQDs have been synthesized under solvothermal condition in the presence of 4-vinylphenylboronic acid and boric acid.[80] Such B-GQDs show strong magnetic resonance and upconversion PL property. In a recent work, S-doped GQDs have been synthesized from organic molecules from durian flesh.[81] Increasing reaction temperature leads to higher doping percentage and consequently longer emission wavelength (from blue to orange).

Surface / Edge Functionalization. Surface passivation (e.g., by PEG) to block traps or defects leads to QY increase.[82] PEG (or PEI) functionalization also red-shifts PL because of bandgap narrowing, resulting from the charge transfer from the functional groups to GQD.[83]

Inspired by the previous studies,[84, 85] Yan et al recently propose two distinct strategies to systematically and continuously narrow down the electronic bandgap of GQDs with an initial wider bandgap (Figure 3f).[86] Because the bandgap of pristine GQD (separation between π and π* orbitals) is inversely proportional to the size of sp^2 domain, bandgap narrowing is realized via conjugating GQDs with polyaromatic molecules to enlarge the π-conjugated sp^2-carbon network. Larger conjugated polyaromatic molecules narrower

the resulting GQD bandgap (hence longer PL emission wavelength). It may be speculated that this strategy will not work as well for CDs or other QDs because their bandgaps are less sensitive to quantum confinement. Alternatively, bandgap narrowing is achieved by introducing an intermediate n-orbital between π and π* orbitals upon grafting with electron-donating chemical groups. The stronger the electron-donating ability of the chemical groups the narrower the resulting GQD bandgap.

4. Applications

4.1. Energy conversion and storage

GQDs promise a wide range of applications in energy conversion and storage because of its large surface area, abundant active sites, capability to facilitate charge transfer and transport, tunable optical properties, and ability to intimately integrate with other nanomaterials.

Photovoltaics. GQDs have served as the sensitizers in GQD/semiconductor solar cells,[87-92, 93] electron/hole transport layer materials in organic or perovskite solar cells[84, 94, 95] and the active layer additive in donor/acceptor blends for dye-sensitized solar cells.[96-98] In the GQD/semiconductor heterojunction based solar cell (Figure 4a), GQDs favor carrier separation,[87, 88] light absorption,[89, 90] charge carrier extraction,[91] and down-conversion property (Figure 4b).[92, 93, 99] A solar cell fabricated by kinetic spray of GQDs onto crystalline-Si shows a high power conversion efficiency of 15.3% partly because a UV photon absorbed by GQD can generate two electrons at the heterojunction (Figure 4c).[89] For organic or perovskite solar cells, GQDs with electron-donating (or electron

withdrawing) functional groups serve well in the electron[84] (or hole[94]) extraction layer by decreasing (or increasing) the work function (Figure 4d).[91] Being sandwiched between perovskite and TiO_2 cathode, the electron-donating phenylenediamine-functionalized GQDs with narrow bandgap enhance electron extraction, and consequently increase the power conversion efficiency by 15.1% compared to the solar cell without GQDs (Figure 4e).[84] When being coated between polymer active layer and ITO anode, the electron-withdrawing COOH-functionalized GQDs enhance hole extraction, and thus improve the power conversion efficiency by 50%.[94] In dye-sensitized solar cells, GQDs promote light absorption,[96] charge separation,[97] and exciton dissociation (Figure 4f).[98] When GQDs being bonded into the active layer by PEG, P3HT as the donor and PCBM as the acceptor, the solar cell exhibits 36% efficiency improvement compared with the solar cell without GQDs.[98]

Light Emitting Diodes (LED). In LEDs, GQDs can serve as the electroluminescent phosphor (Figure 5a-b),[8, 100, 101, 102] dopant in organic light emitter,[38] bandgap tuner,[37] or color converter.[103, 104] As the electroluminescent phosphor, octadecylamine-functionalized GQD (ODA-GQD) based LED achieves the highest current (6.51 cd/A) and external quantum efficiency (2.67%) among the reported GQD-based LEDs, because ODA-GQDs reduce the hole barrier and improve the hole injection efficiency from anode to active layer.[102] As the dopant in organic light emitter, GQDs with narrower bandgap offer brighter white electroluminescence because narrow bandgap favors low-energy emission and reduces exciton lifetime (Figure 5c-d).[38] As the bandgap tuner in active layer, GQDs functionalized with electron-donating aniline derivatives exhibit red-shifted

electroluminescence because of bandgap narrowing, and consequently improve color purity (Figure 5e).[37] As the color converter, amino-functionalized GQDs casted on blue LED chip convert blue light to white (Figure 5f).[104]

Photodetectors. Taking advantage of the good light adsorption of GQDs, they have been used as photosensitizers in photodectors (Figure 6a).[105, 106] Large-bandgap GQDs have been used to form heterostructure for highly selective UV detection (Figure 6b).[107-109] The excellent responsivity of 36 A/W, detectivity of 1.3×10^{12} $Hz^{1/2}/W$, and ultrasensitive response of 7.0 mA/cm^2 under weak UV light (0.07 mW/cm^2) have been achieved by GQD decorated ZnO nanorods (Figure 6c).[109] The authors also demonstrate that GQDs are superior to carbon dots due to their lower trap-state density and the better ability to lower the energy barrier. GQD and graphene hybrid supported on lead zirconate titanate (PZT) makes a stable, rapid and ultrasensitive (4.06×10^9 A/W) photodetector for broadband light detection.[110] The built-in electric field induced by PZT favors separation of electron-hole pairs and subsequent hole transfer to the underlying graphene channel. Narrow-bandgap GQDs have been used to widen the light adsorption range. Diaminonaphthalene-functionalized GQDs with much reduced bandgap (1.3 eV) have been hybridized with graphene and coated on boron nitride sheets to provide photodetection from UV to infrared (Figure 6d).[111] Polymer (e.g. PEI,[105] PANI[112]) functionalization induces multiple trap states on GQD which favor the realization of broadband photodetector.

Thermoelectric devices. In thermoelectric devices, GQDs have been employed to restrict thermal conductivity[113] and the size of thermoelectric nanocrystals by acting as

the capping agent.[114] Specifically, GQDs have been utilized as the ligand exchanger to stabilize PbTe, PbSe, PbS and CdSe nanoparticles, preventing their overgrowth and aggregation.[114] GQDs preserve quantum confinement of the nanocrystals and promote energy filtering of carriers. The device achieves the figure of merit (ZT) of 0.46 at 650 K. GQDs/Bi_2Te_3 hybrid nanosheets show reduced thermal conductivity than Bi_2Te_3 alone because GQDs with oxygenated groups increase the interface coulomb barriers and power factor.[113] With GQD size of 20 nm, the optimized ZT of 0.55 is attained at 425 K, which is much higher than that of pristine Bi_2Te_3.

Supercapacitors. GQDs have been used for supercapacitors, because of their large specific surface area (Figure 7a)[115] and high pseudo-capacitance originated from edges,[116] defects,[117] functional groups,[118] and dopants (Figure 7b).[119, 120] N-doped GQDs[121] and amine-functionalized GQDs[122] have achieved high specific capacitance of 509 and 595 F/g, respectively. It has also been demonstrated that decoration of GQDs can largely enhance the capacitance of 3D graphene (Figure 7c).[123] A flexible and transparent GQD-graphene micro-supercapacitor shows specific capacitance of 9.09 $\mu F/cm^2$ with high stability.[124] Hybridized GQD-polyaniline nanotubes exhibit a high specific capacitance of 1044 F/g due to the large surface area and conductivity.[125] A heterostructure electrode is fabricated by growing GQDs on MnO_2 nanosheets using chemical vapor deposition, with good interface bonding due to formation of Mn-O-C bonds (Figure 7d).[116] GQDs extend the potential window to 1.3 V because of built-in electric field resulting from the different work functions of the two materials. The

specific capacitance reaches 1170 F/g at a scan rate of 5 mV/s, which is the highest among all GQD-based supercapacitors.

Rechargeable batteries. In Li or Na ion batteries, GQDs can help to relieve the volume expansion,[126] accelerate Li^+/Na^+ diffusion[127, 128] and electron transfer,[129, 130] enhance the interfacial double layer,[131, 132] and improve electrochemical properties.[126, 129, 131, 133] GQDs have been used as the surface sensitizer on VO_2/graphene arrays to enhance electrochemical performance, whereby enabling a high Li-battery capacity (>420 mAh/g) and Na-battery capacity (306 mAh/g) at 18 A/g with high stability (Figure 8a).[131] GQDs can expand interlayer distance between MoS_2 layers and hence accelerate electrochemical kinetics with high stability.[126] GQDs/MoS_2 exhibits high discharge capacity of 820 mAh/g at 2 A/g, which is 2.5 times higher than the electrode made of MoS_2 only. Coating of phenylalanine-functionalized GQDs on Si electrode accelerates electron transfer and Li^+ diffusion, achieving a high capacity of 1820 mAh/g at 1A/g.[129] Because GQDs inhibit ion-solvent clustering and immobilize PF_6^- anions to enhance the Li^+ diffusion and conductivity, $LiFePO_4$ battery based on GQD modified gel polymer electrolyte delivers a high capacity of 155 mAh/g at 0.1 C and exhibit a long cycle life up to 500 cycles at 5 C.[127] GQDs can also enhance Li^+ diffusion by immobilizing S_n^{2-} in a lithium–sulfur battery (Figure 8b).[128]

4.2. Catalysis

Chemical groups and dopants confer GQDs with intrinsic catalytic properties. They can also improve the performance of many catalysts through bandgap alignment, synergic

cooperation, morphology modulation, light adsorption enhancement, or promotion of charge transfer. Owing to their chemical inertness, GQDs often can enhance the stability of other catalysts. Because GQDs are highly dispersible, they may act as quasi-homogeneous catalysts providing both high catalytic efficiency and possibility to be recycled, in other words, combining the merits of homogeneous and heterogeneous catalysts.

Photocatalysis. Making use of fully accessible surface, tunable bandgap structure, good light absorption, high dispersibility, excellent photostability, and the ability to form heterojunction with other nanomaterials, GQDs have been employed as photocatalysts for H_2 evolution,[24-26, 86, 134-138] CO_2 reduction[86, 139, 140] and pollutants degradation.[74, 79, 141, 142, 143-146] GQDs are desirable photocatalysts because their typical bandgaps (1.8 – 2.4 eV) are large enough to drive redox reactions and yet not too large to ensure broad light adsorption. And light adsorption range and exciton separation may be enhanced by forming heterojunctions or hybrids with other light harvesting nanomaterials.

The electron-donating moieties (dopants such as N and S or chemical groups such as –NH_2) and electron-withdrawing moieties (chemical groups such as –COOH) on a GQD induce n- and p-type conductivity respectively, while the basal carbon network acts as Ohmic contact between them. This can be regarded as the unique intramolecular Z-scheme structure (Figure 9a)[86] or intramolecular p-n type photochemical diode.[24] Such structure favours separation of photogenerated electron-hole pairs and enables simultaneous occurrence of oxidation reaction at n-type domains and reduction reaction

at p-type domains. A GQD with engineered narrow bandgap (thus enhanced light adsorption) and intramolecular Z-scheme has been used for efficient CO_2 reduction and H_2 evolution.[86] A N-doped GQD with oxygenated groups (Figure 9b)[25] and a S-doped GQD with oxygenated groups[137] have also shown good performance in H_2 evolution. GQDs have been hybridized with other nanomaterials (TiO_2,[134] CdS,[136] $ZnNb_2O_6$/g-C_3N_4[135]) for H_2 evolution, serving as the light absorber or/and electron acceptor in the heterojunction. For example, the heterojunction formed between S, N co-doped GQD and TiO_2 exhibits an ultrahigh photocatalytic H_2 evolution rate of 86 mmol g_{cat}^{-1} h^{-1}.[138]

A chromophore-functionalized GQD coupled with formate dehydrogenase shows high formic acid formation rate of 99.48 μmol h^{-1} from CO_2 reduction because such photocatalyst–biocatalyst integrated system can utilize light energy from UV to NIR.[139] Hybridization of N-doped GQDs with perovskite nanocubes (nitrogen and oxygen vacancy confined in sodium tantalite, Vo-NaTaON) provides excellent photo-reduction rates of CO_2 towards CO and CH_4 at 43 and 14 μmol $g_{cat}^{-1}h^{-1}$ respectively, due to enhanced light absorption and charge separation (Figure 9c).[140]

Doped GQDs have been used as the photocatalysts for organic synthesis too. For example, a N, S co-doped GQD displays high photocatalytic performance in aerobic oxidative coupling of various amines (100% conversion) owing to broad light adsorption, increased electron-rich Fermi level, and prolonged lifetime of the excited singlet state to convert oxygen to superoxide.[49] A hybrid of N, S co-doped GQD and Fe(III) tetra(4-sulfonatophenyl)porphyrins shows good performance in selective photo-oxidation of

alcohols to desired carbonyl compounds attributable to enhanced light absorption, charge separation and oxygen activation.[147]

GQDs have been utilized for photocatalytic degradation of pollutants, making use of their light adsorption and ability to form heterojunction (e.g., with zinc porphyrin,[141] TiO_2,[79, 142] Bi_2MoO_6,[144] C_3N_4,[145, 146] $MnNb_2O_6$,[74] or N-$Bi_2O_2CO_3$[148] as shown in Figure 9d) or form Z-scheme structure (e.g., with ZnO[143]). For instance, GQD-zinc porphyrin heterojunction with improved separation of electron-hole pairs promotes generation of superoxide anion radical or H_2O_2 for faster degradation of methylene blue (MB).[141] Similarly, GQD/C_3N_4 heterojunction can produce more superoxide anion radical and holes for better photocatalytic degradation of rhodamine B (RhB) and tetracycline (TC), (Figure 9e).[145]

Electrocatalysis. GQDs are instrumental for electrocatalytic reactions, such as oxygen reduction (ORR),[45, 149-155, 156] oxygen evolution (OER),[157-160] hydrogen evolution (HER)[19, 161-163] and CO_2 reduction[164-166] reactions. B,N-GQDs[153] and N-GQDs[154] have been employed as ORR catalysts based on their catalytically active dopant sites. But usually, GQDs are hybridized with other nanomaterials such as graphene,[45, 151, 152] C_3N_4,[149] carbon nanotubes,[150] and reduced graphene oxide (rGO)[155, 156] to realize synergistic effects. Because of abundant active sites (edges, defects, and interfaces) and fast charge transfer between GQDs and graphene nanoribbons (GNRs), GQD-GNR hybrid demonstrates ultrahigh performance for ORR with high selectivity and stability, as well as higher limiting current density and lower overpotential than those of Pt.[45] Hybrid

of B, N-GQD and graphene combines the catalytic abilities of the former and the high conductivity of the latter, leading to excellent ORR performance far superior to commercial Pt/C.[152] MoS_2-rGO 3D framework decorated with N-GQDs has been used for direct methanol fuel cells with excellent ORR performance, stability and methanol tolerance.[156]

N-GQDs are good electrocatalysts for OER because N dopants induce charge redistribution through π-π delocalization to reduce *OOH thermodynamic energy barrier.[160] But often, GQDs are hybridized with nanomaterials such as $NiCo_2P_2$,[157] Ni_3S_2[158] and Co_3O_4[159] to improve the performance.[160] It has recently been demonstrated that GQDs are able to engineer nano-catalysts into nanosheet morphology because of their atomically thin planar structure (Figure 9f).[5] Specifically, GQDs greatly boost both OER and HER performance of $NiCo_2P_2$ by controlling catalyst morphology, enhancing charge transfer and transport, and improving the catalytic kinetics.[157] GQDs have also been used to improve the HER performance of MoS_2,[19, 161] Ni_3S_2,[162] and CoP.[163] GQD-MoS_2 composite can achieve high HER activity with low onset potential and good stability because GQDs reduce the bandgap toward zero and enhance charge transfer.[19] Depositing GQDs on CoP nanoparticles grown on graphene (GQDs/CoP/G) gives nearly 100% Faradaic efficiency in HER, because of increased active surface area, promoted conductivity and carrier mobility.[163]

N-doped GQDs can electrocatalyze CO_2 reduction into hydrocarbons and oxygenates at high current density, good Faradaic efficiency (90%) and low overpotential, with

selective conversion (45%) toward ethylene and ethanol.[164] In contrast, undoped GQDs and N-doped rGOs mainly produce CO and $HCOO^-$ through distinct reaction routes, testifying the importance of N-doping and the superiority of GQD to rGO. DFT calculations show that N dopants on a GQD electrochemically convert CO_2 into CH_4, C_2H_4, C_2H_5OH, $HCOO^-$ and CO at <-0.6 V.[165] N dopants also facilitate adsorption of reaction intermediate (*COOH) whereby promoting reduction of CO_2 to CO. Desirably, the presence of water favors the reaction selectivity towards CH_4. A well-defined GQD-Rhenium complex as a molecular catalyst exhibits a ultralow overpotential (-0.48 V vs NHE) for CO_2 reduction to CO (Figure 9g).[166] N-GQDs decorated Bi_2O_3 nanosheets show ~100% Faraday efficiency for reduction of CO_2 to formate at an overpotential of 0.7 V, owing to the enhanced adsorption ability of CO_2 by N-GQDs.[167]

GQDs are also useful for electrocatalytic organic synthesis and fuel cells. As an example, metal/GQD composites prepared through layer-by-layer assembly exhibit efficient and versatile catalytic capability in selective conversion of aromatic nitro compounds, methanol electro-oxidation and water splitting, attributable to the increased charge transfer and synergistic interaction between metal (Au, Ag, Pt) nanocrystals and GQDs.[168]

Photoelectrocatalysis. GQDs have been used as photosensitizer,[169, 170] electron donor[171] or hole extractor[171, 172] for photoelectrochemical reactions. GQDs modified ZnO nanowires functionalized with 3-aminopropyltriethoxysilane (GQDs@APTES-ZnO NWs) can work as photoanode for photoelectrochemical water splitting with much

increased efficiency, owing to GQD-enhanced light absorption and charge separation.[169] As a chemically inert carbon material, GQD improves the stability of CdSe QD-sensitized photoanode.[171] At the same time, as the hole extractor and electron donor, it accelerates charge transfer kinetics for photoelectrochemical degradation of MB and hydrogen evolution.

Chemical Catalysis. The chemical groups on a GQD are able to catalyze chemical reactions. It has been recently demonstrated that GQDs bearing $–SO_3H$ and –COOH groups can serve as the highly effective and recyclable quasi-homogeneous acid catalyst for one-pot selective conversion of carbohydrates into 5-hydroxymethylfurfural.[60] The high efficiency is partly attributable to the cooperation between different functional groups on GQDs. It is conceivable that GQDs with various chemical groups, dopants, or decorated nano-catalysts (e.g., Pt nanoparticles) shall be able to catalyze more complex reactions or multi-step reactions at one site.

GQDs can act as the peroxidase mimics to convert H_2O_2 into hydroxyl radicals. It has been shown that -C=O groups on GQD are the catalytic sites while O=C–O– groups are the substrate-binding sites.[59] Utilizing such enzymatic activity and its ability to tightly bind with aromatic alcohols via π-π interaction, Au/GQD nanoparticles have shown high performance in oxidizing veratryl alcohol to veratryl aldehyde or veratric acid, in the presence of H_2O_2.[173]

4.3 Flexible devices

Considering their small size and exceptional mechanical properties (e.g. both high strength and flexibility), GQDs are naturally suitable for flexible devices. Given their high dispersibility, they are particularly attractive for printable flexible devices.

Flexible memory devices. GQDs are able to function as the charge-trap material in memory devices, owing to their multiple energy levels, edge states and quantum confinement effect.[174-176] Or they can be used as resistive switching material based on the resonant electron tunneling effect.[177] GQDs coated between SiO_2 layers work as the charge-traps for memory capacitor.[174] The memory window, program and erase speed, durability and data-retention can be modulated by GQD size. When GQDs are used as charge trapping medium for organic nano-floating gate memory, highly reversible switching performance with the on/off current ratio more than 10^6, long retention time over 10^4 s and cycle endurance >100 have been achieved.[175] The GQD layer is able to trap charges as high as 7.2×10^{12} per cm^2.

Flexible electrochromic devices. GQDs have been applied in flexible electrochromic devices, serving as electron transfer medium to replace electrolyte solution. A electrolyte-free flexible electrochromic device using the composite of GQD and methyl viologen displays a stable switching performance, high endurance and stability.[178]

4.4 Biomedical Applications

It is not surprising that GQDs are highly biocompatible to carbon-based life on earth. And comparing to other nanomaterials or their nanocarbon cousins, GQDs have much

fast renal clearance and bio-degradation rate due to their small sizes. Their unique optical, electrochemical, and physicochemical properties enable many theranostic applications. Applications of GQD-based sensors for monitoring food safety are also discussed in this section.

Cellular and in vivo Imaging. Because of photobleaching, conventional organic fluorophores do not allow long-term imaging. To tackle this issue, semiconductor quantum dots have been widely used. However, being much bigger than a biomolecule, semiconductor QDs may alter the dynamics (functions) of the target and bind with multiple targets to create artificial cluster. Besides, they can be toxic due to leaching of heavy metal ions. In comparison, GQDs offer unique advantages for molecular imaging in cells owing to the unique combination of several key merits, including good photostability, molecular size, biocompatibility, ease to be functionalized, tunable PL properties, good dispersibility, and chemical stability.[2]

Since the first demonstration of GQD for molecular (insulin receptor) imaging and dynamic tracking in live cells,[179] there are several new developments worthy to be highlighted. Instead of conjugating GQDs with proteins or other recognition moieties, Chen et al for the first time functionalize GQD with monosaccharaides to reveal the distribution and trafficking of carbohydrate receptors on cells.[180] Recently, Li et al have devised a reversible fluorescence probe sensitive to both oxidants and reductants and used such GQD probe for real-time monitoring of dynamic change in intracellular redox state in response to oxidative or reductive stress (Figure 10a).[181] This is the first

demonstration of using GQDs to examine a cellular dynamic activity. Later, the same authors demonstrated a GQD-based fluorescence probe for real-time monitoring of triggered dynamic change of the intracellular H_2S level in live cells.[182] Unlike most GQD-based probes, this is a fluorescence turn-on probe, functionalized with electron-withdrawing dinitrophenyl groups which quench GQD PL through photoinduced electron transfer and can be specifically cleaved by H_2S to allow recovery of GQD PL.

GQDs that emit long wavelengths or be excited by long wavelengths residing within the "biological transparent windows" (650-950 nm and 1000-1350 nm) are particularly attractive for in vivo imaging. Red fluorescence GQDs can be made by doping heteroatoms to narrow the bandgap. For examples, a S,N co-doped GQD emitting at 640 nm has been used for cellular imaging (Figure 10b)[138] and a S-doped GQD emitting at 680 nm has been used for in vivo imaging in mice (Figure 10c).[72] Another 680 nm emitting GQD prepared from a mango leaf has been used for cell imaging.[183] Heteroatom doping may confer GQDs with extraordinary PL properties. A N,P co-doped GQD exhibits strong two-photon upconversion property.[52] A B-doped GQD which has two-photon upconversion and magnetic property has been employed for both NIR and MRI imaging (Figure 10d).[80] The two-photon upconversion property provides the possibility for in vivo deep-tissue imaging. A N-doped GQD has been employed for two-photon imaging in mice with 800 nm excitation.[184] In another example, N-doped GQD conjugate has been utilized to reveal endogenous H_2O_2 level in mice based on quenching of two-photon PL emission under 740 nm excitation.[185] GQDs functionalized with peptide[186] or alkylamines[187] also show up-conversion PL for NIR excited imaging.

Photoluminescence sensing. Owing to their small size, PL of GQDs is extremely sensitive to minute environmental perturbation and they can intimately interact with small molecules. Therefore, GQD based luminescence sensors often provide much improved sensitivity.[2] Various sensors have been developed making use of the fact that PL of molecularly-sized GQDs is particularly sensitive to aggregation-induced PL quenching,[188, 189] fluorescence resonance energy transfer (FRET),[190] photon-induced electron transfer,[181, 191] or PL increase in presence of turn-on chromoionophore.[192] For example, Li et al have demonstrated specific fluorometric assay of multiple metabolites in a blood droplet using tyramine-functionalized GQDs (Figure 11a).[189] In this system, GQD acts not only as fluorescence reporter but also as hydrogen peroxidase mimic which produces free radicals from enzymatically generated H_2O_2 to induce GQD crosslinking (hence aggregation). Also based on GQD aggregation induced PL quenching, Shen et al have demonstrated highly luminescent N, S co-doped GQDs for parallel detection of Fe^{3+}, Cu^{2+} and Ag^{+} ions with low detection limits because of the coordination reaction between these ions and the heteroatoms / functional groups on GQDs (Figure 11b).[15] GQD based PL sensors have been used to detect food poisoning, including bacteria,[193] insecticides,[194] heavy metal ions,[195] food packaging materials.[196] For example, a turn-on fluorescence sensor based on N and S co-doped GQDs has been used to detect ethion (insecticide) in food samples.[197] Firstly GQD PL is quenched by Hg^{2+} due to charge transfer through Hg-S bonds. In the presence of ethion, GQD PL recovers because Hg^{2+} is deprived from GQD by this S-containing small molecule.

Electrochemiluminescence (ECL) Sensing. Generally, ECL sensing is based on excitation of GQDs by the radicals electrochemically derived at the electrode surface from a co-reactant (Figure 11c).[21] When charge transfer between GQDs and radicals is interrupted by the targeted analytes, ECL is quenched in a dose-dependent manner. Using cathodic ECL and $S_2O_8^{2-}$ as the co-reactant, sensitive detection of metal ion,[21, 198] protein[199] and nucleic acids (Figure 11d)[200, 201] has been demonstrated. Using anodic ECL and H_2O_2 as the co-reactant, pH[202, 203] and Co^{2+} ion[203] are detected with high sensitivity.

Electrochemical Sensing. Using GQD's ability to specifically and intimately interact with small analytes (via π-π interaction or interaction with functional moieties or dopants on GQDs), facilitate charge transfer, and catalyze redox species, they have been used for electrochemical detection of metal ions,[204, 205] dopamine,[205, 206] epinephrine,[207] H_2O_2,[208] glutathione,[66] alkaline phosphatase,[209] endogenous arachidonic acid,[210] pesticide[211] and therapeutic drugs.[212] A novel electrochemical sensing platform based on nanochannel confined GQDs has recently been demonstrated (Figure 11e),[205] where GQD serves as the signal recognition element through specific interaction with the analytes (coordination with metal ions by its functional groups or dopants, π-π interaction with dopamine) and as the signal enhancer through electrostatic enrichment of the analytes and facilitation of charge transfer. Meanwhile, the vertically-aligned nanochannel array prevents non-specific access to the electrode by numerous molecules in the complex fluid samples. This sensor is able to detect heavy metal ions with ultralow

detection limits (9.8 pM for Hg^{2+}, 8.3 pM for Cu^{2+}, and 4.3 nM for Cd^{2+}) in the complex practical samples (serum and seafoods) without the need of tedious pretreatments.

Photoelectrochemical sensing is based on the enhancement of photocurrent when the interaction between the analyte and the photoresponsive material consumes photogenerated holes at anode[213] or photogenerated electrons at cathode.[214] For instance, using GQD coated TiO_2 nanoparticles, sensitive detection (limit of 6.7 nM) of dopamine (having pi-pi interaction with GQD) has been demonstrated.[213] As another example, a N-GQD/ I-BiOCl cathode offers a low detection limit of 0.01 ng/mL for chlorpyrifos.[215]

Photothermal and Photodynamic Therapy. As a new kind of photothermal and photodynamic therapy agent, GQD exhibits some unique advantages such as good biocompatibility, excellent dispersibility, broad light absorption, good photostability, fast body clearance, ease to be degraded by enzymes, and the ability to produce radicals.[42, 216] A N-GQD with good photothermal conversion efficiency of 62.53% has been reported.[217] IR780 is an excellent NIR photothermal agent, but suffers from poor solubility. Folic acid functionalized GQDs can hybridize with IR780 through π-π stacking and the hybrid shows excellent dispersibility and much enhanced photothermal conversion efficiency of 87.9% due to synergistic effects (Figure 12a).[218]

GQDs have been used for photodynamic therapy (Figure 12b)[219] and killing bacteria[220] because they can produce reactive oxygen species (ROS) under light irradiation.[221] A

COOH-bearing GQD demonstrates good photodynamic property under NIR two-photon excitation, promising for deep tissue cancer therapy.[222] It has been shown that N-doping enhances GQD's ability to generate singlet oxygen and superoxide radical anions.[223] And such N-doped GQD has been employed for in vivo cancer therapy under NIR two-photon excitation. Ge et al. reported a N, S-doped GQD which has an excellent $^1O_2$ quantum yield of 1.3 owing to a multistate sensitization mechanism under visible light illumination.[72] In vivo and in vitro studies demonstrate its potential for treating skin cancers.

Other therapeutic applications. GQDs conjugated with an antiretroviral agent (CHI499) is able to suppress HIV based on inhibition of both the activity of reverse transcriptase and virus binding to the cells.[224] GQDs have also show potential to treat Parkinson's disease via inhibiting fibrillization of α-syn and directly disaggregating the mature fibrils.[225] Furthermore, GQDs can rescue neuronal death and synaptic loss, reduce Lewy body and Lewy neurite formation, ameliorate mitochondrial dysfunctions, and prevent neuron-to-neuron transmission of α-syn pathology provoked by α-syn preformed fibrils. For amyloidosis treatment, the electrostatic and π-π interactions between GQDs and islet amyloid polypeptide (IAPP) prevents the aggregation and toxicity of IAPP fibrils.[226]

5. Current Challenges and Outlook

GQDs are flat 0D nancarbon materials which could change the landscape in many fields of science and technology. Although the development is rapid, there are still issues to be addressed and challenges to be overcome. First of all, in order to have a roadmap of GQD

research, its unambiguous definition should be agreed upon by the community and its unique properties distinct to similarly structured nanomaterials should be recognized, otherwise confusions and inconsistencies will be resulted in the literature and GQD applications are not optimal. In addition, it should be kept in mind that owing to the large heterogeneity in composition, size, and shape, GQDs prepared by different methods cover a very wide range of chemicophysical properties. Therefore, a successful application based on one kind of GQD may not be feasible to another kind. An urgent need is to develop methods to synthesize GQDs with well-defined characteristics or to precisely engineer GQD properties or to differentially isolate different GQD populations, so that, better and more systematic characterization and understanding of GQDs, as well as more effective applications can be achieved.

For imaging, display and fluorescence-based sensing, the disadvantage of GQD is the relatively low PL QY as compared to other fluorophores such as CDs, semiconductor QDs, and organic dyes. QY can be improved by removing or passivating the chemical moieties acting as the non-radiative recombination centers and introducing heteroatom doping. Some GQDs have QY >30% which is high enough for most bioimaging purposes. Although it is unlikely GQD can be as bright as some of its competitors (keeping in mind that GQD is very small), its other merits together warrant many unique applications.

GQD may be viewed as a complex giant π-conjugated molecule whose properties are influenced by many factors, such as, size, chemical groups, dopants, edge configurations, defects, and shape. Experimentally isolating their individual influence is challenging

without being able to precisely control GQD composition and morphology, whereas theoretical studies can provide important insights.[62] Currently, little is known about the interplay between these factors (e.g., co-existence of both electron-donating and electron-withdrawing chemical groups and co-existence of different heteroatom dopants). These interplays shall bring new properties thus new application opportunities. In addition, heterojunctions formed between GQDs and other nanomaterials are not thoroughly studied although interesting phenomena have already been observed and more are highly anticipated. An interesting study shows that chirality can be introduced to a GQD by edge-functionalization of chiral molecules.[227] How chirality or distortion in general affects GQD properties deserves further investigation.

The current scope of GQD applications has already covered a wide range of topics. And it is still expanding, for examples, the recent use of GQDs as quasi-homogeneous catalysts for chemical synthesis and conversion[60] and use of GQDs for flexible devices.[176] Just like other graphene materials, GQDs can be used to engineer and improve the properties of other functional nanomaterials.[5] Conceivably, in view of their high dispersibility and intrinsic amphiphilic properties, GQDs may serve as a new class of surfactants for many applications.

Currently, many applications of GQDs are not practically feasible because low-cost industrial-scale synthesis of GQDs has not been actually realized yet. But we predict that just like the current capability for mass-production of graphene materials, ton-scale production of GQDs are possible using either top-down or bottom-up strategies. Not only

the synthesis but also purification should be scalable. On benchtop, ultrafiltration is often used for purification which is faster than also commonly used methods like dialysis and electrophoresis. But it is expensive and not feasible for large-scale production. In comparison, cross-flow ultrafiltration is suitable for industrial production and ensure constant throughput because of the absence of buildup on the membrane. On the other hand, mass-production is not a major hurdle to biomedical applications or some applications that only require a small amount of GQDs as the additives. In our opinion, GQD research is still young yet has a great potential if current challenges can be tackled and the unique combination of desirable merits of GQDs can be properly utilized.

Acknowledgements

This research was supported by AcRF tier 2 grants (MOE2017-T2-2-005) from Ministry of Education (Singapore).

References

[1] X. W. Wang, G. Z. Sun, N. Li, P. Chen, Chemical Society Reviews 2016, 45, 2239.
[2] X. T. Zheng, A. Ananthanarayanan, K. Q. Luo, P. Chen, Small 2015, 11, 1620.
[3] L. Li, G. Wu, G. Yang, J. Peng, J. Zhao, J.-J. Zhu, Nanoscale 2013, 5, 4015.
[4] M. A. Sk, A. Ananthanarayanan, L. Huang, K. H. Lim, P. Chen, Journal of Materials Chemistry C 2014, 2, 6954.
[5] J. Tian, J. Chen, J. Liu, Q. Tian, P. Chen, Nano Energy 2018, 48, 284.
[6] K.-A. Tsai, Y.-J. Hsu, Applied Catalysis B: Environmental 2015, 164, 271.
[7] Z. Zeng, S. Chen, T. T. Y. Tan, F.-X. Xiao, Catalysis Today 2018, 315, 171; Z. Zhang, J. Zhang, N. Chen, L. Qu, Energy & Environmental Science 2012, 5, 8869; P. Tian, L. Tang, K. S. Teng, S. P. Lau, Materials Today Chemistry 2018, 10, 221.
[8] Z. M. Luo, G. Q. Qi, K. Y. Chen, M. Zou, L. H. Yuwen, X. W. Zhang, W. Huang, L. H. Wang, Advanced Functional Materials 2016, 26, 2739.
[9] S. H. Jin, D. H. Kim, G. H. Jun, S. H. Hong, S. Jeon, Acs Nano 2013, 7, 1239.

[10] H. Yoon, Y. H. Chang, S. H. Song, E. S. Lee, S. H. Jin, C. Park, J. Lee, B. H. Kim, H. J. Kang, Y. H. Kim, S. Jeon, Advanced Materials 2016, 28, 5255.
[11] J. Ali, G.-u.-d. Siddiqui, Y. J. Yang, K. T. Lee, K. Um, K. H. Choi, RSC Advances 2016, 6, 5068.
[12] P. Herwig, C. W. Kayser, K. Müllen, H. W. Spiess, Advanced Materials 1996, 8, 510; A. Fechtenkötter, K. Saalwächter, M. A. Harbison, K. Müllen, H. W. Spiess, Angewandte Chemie International Edition 1999, 38, 3039; L. Zhi, K. Müllen, Journal of Materials Chemistry 2008, 18, 1472.
[13] X. Wu, F. Tian, W. X. Wang, J. Chen, M. Wu, J. X. Zhao, Journal of Materials Chemistry C 2013, 1, 4676.
[14] L. Wang, Y. Wang, T. Xu, H. Liao, C. Yao, Y. Liu, Z. Li, Z. Chen, D. Pan, L. Sun, M. Wu, Nature Communications 2014, 5, 5357.
[15] C. Shen, S. Y. Ge, Y. Y. Pang, F. N. Xi, J. Y. Liu, X. P. Dong, P. Chen, Journal of Materials Chemistry B 2017, 5, 6593.
[16] Y. Dong, C. Chen, X. Zheng, L. Gao, Z. Cui, H. Yang, C. Guo, Y. Chi, C. M. Li, Journal of Materials Chemistry 2012, 22, 8764.
[17] Y. Q. Dong, C. Q. Chen, X. T. Zheng, L. L. Gao, Z. M. Cui, H. B. Yang, C. X. Guo, Y. W. Chi, C. M. Li, Journal of Materials Chemistry 2012, 22, 8764.
[18] J. Peng, W. Gao, B. K. Gupta, Z. Liu, R. Romero-Aburto, L. H. Ge, L. Song, L. B. Alemany, X. B. Zhan, G. H. Gao, S. A. Vithayathil, B. A. Kaipparettu, A. A. Marti, T. Hayashi, J. J. Zhu, P. M. Ajayan, Nano Letters 2012, 12, 844.
[19] B. Guo, K. Yu, H. Li, R. Qi, Y. Zhang, H. Song, Z. Tang, Z. Zhu, M. Chen, ACS applied materials & interfaces 2017, 9, 3653.
[20] S. Zhuo, M. Shao, S.-T. Lee, Acs Nano 2012, 6, 1059; D. Pan, J. Zhang, Z. Li, M. Wu, Advanced Materials 2010, 22, 734.
[21] L. L. Li, J. Ji, R. Fei, C. Z. Wang, Q. Lu, J. R. Zhang, L. P. Jiang, J. J. Zhu, Advanced Functional Materials 2012, 22, 2971.
[22] S. Chen, J. W. Liu, M. L. Chen, X. W. Chen, J. H. Wang, Chemical Communications 2012, 48, 7637.
[23] G. Rajender, P. K. Giri, Journal of Materials Chemistry C 2016, 4, 10852.
[24] T. F. Yeh, C. Y. Teng, S. J. Chen, H. Teng, Advanced Materials 2014, 26, 3297.
[25] L. C. Chen, C. Y. Teng, C. Y. Lin, H. Y. Chang, S. J. Chen, H. Teng, Advanced Energy Materials 2016, 6, 1600719.
[26] T. F. Yeh, S. J. Chen, H. S. Teng, Nano Energy 2015, 12, 476.
[27] B. T. Liu, J. Xie, H. Ma, X. Zhang, Y. Pan, J. W. Lv, H. Ge, N. Ren, H. Q. Su, X. J. Xie, L. Huang, W. Huang, Small 2017, 13, CP16.
[28] R. Q. Ye, C. S. Xiang, J. Lin, Z. W. Peng, K. W. Huang, Z. Yan, N. P. Cook, E. L. G. Samuel, C. C. Hwang, G. D. Ruan, G. Ceriotti, A. R. O. Raji, A. A. Marti, J. M. Tour, Nature Communications 2013, 4, 2943.
[29] Y. Shin, J. Park, D. Hyun, J. Yang, J.-H. Lee, J.-H. Kim, H. Lee, Nanoscale 2015, 7, 5633.
[30] Q. Liu, J. Zhang, H. He, G. Huang, B. Xing, J. Jia, C. Zhang, Nanomaterials 2018, 8, 844; R. B. Tian, S. T. Zhong, J. Wu, W. Jiang, Y. W. Shen, T. H. Wang, Optical Materials 2016, 60, 204; F. Jiang, D. Q. Chen, R. M. Li, Y. C. Wang, G. Q. Zhang, S. M. Li, J. P. Zheng, N. Y. Huang, Y. Gu, C. R. Wang, C. Y. Shu, Nanoscale 2013, 5, 1137; C. C. Ke, Y. C. Yang, W. L. Tseng, Particle & Particle Systems Characterization 2016, 33, 132; C. Zhu, S. Yang, G. Wang, R. Mo, P. He, J. Sun, Z. Di, Z. Kang, N. Yuan, J. Ding, G. Ding, X. Xie, Journal of Materials Chemistry B 2015, 3, 6871.

[31] X. Zhou, Y. Zhang, C. Wang, X. Wu, Y. Yang, B. Zheng, H. Wu, S. Guo, J. Zhang, ACS Nano 2012, 6, 6592.
[32] A. Ananthanarayanan, X. W. Wang, P. Routh, B. Sana, S. Lim, D. H. Kim, K. H. Lim, J. Li, P. Chen, Advanced Functional Materials 2014, 24, 3021.
[33] D. B. Shinde, V. K. Pillai, Chemistry-a European Journal 2012, 18, 12522.
[34] M. Zhang, L. L. Bai, W. H. Shang, W. J. Xie, H. Ma, Y. Y. Fu, D. C. Fang, H. Sun, L. Z. Fan, M. Han, C. M. Liu, S. H. Yang, Journal of Materials Chemistry 2012, 22, 7461; Z. M. Markovic, B. Z. Ristic, K. M. Arsikin, D. G. Klisic, L. M. Harhaji-Trajkovic, B. M. Todorovic-Markovic, D. P. Kepic, T. K. Kravic-Stevovic, S. P. Jovanovic, M. M. Milenkovic, D. D. Milivojevic, V. Z. Bumbasirevic, M. D. Dramicanin, V. S. Trajkovic, Biomaterials 2012, 33, 7084; F. L. Yuan, L. Ding, Y. C. Li, X. H. Li, L. Z. Fan, S. X. Zhou, D. C. Fang, S. H. Yang, Nanoscale 2015, 7, 11727.
[35] M. He, X. Guo, J. Huang, H. Shen, Q. Zeng, L. Wang, Carbon 2018, 140, 508.
[36] H. Huang, S. Yang, Q. Li, Y. Yang, G. Wang, X. You, B. Mao, H. Wang, Y. Ma, P. He, Z. Liu, G. Ding, X. Xie, Langmuir 2018, 34, 250.
[37] W. Kwon, Y. H. Kim, J. H. Kim, T. Lee, S. Do, Y. Park, M. S. Jeong, T. W. Lee, S. W. Rhee, Scientific Reports 2016, 6, 24205.
[38] W. Kwon, Y. H. Kim, C. L. Lee, M. Lee, H. C. Choi, T. W. Lee, S. W. Rhee, Nano Letters 2014, 14, 1306.
[39] H. Tetsuka, R. Asahi, A. Nagoya, K. Okamoto, I. Tajima, R. Ohta, A. Okamoto, Advanced Materials 2012, 24, 5333.
[40] G. S. Kumar, R. Roy, D. Sen, U. K. Ghorai, R. Thapa, N. Mazumder, S. Saha, K. K. Chattopadhyay, Nanoscale 2014, 6, 3384.
[41] Q. Liu, B. D. Guo, Z. Y. Rao, B. H. Zhang, J. R. Gong, Nano Letters 2013, 13, 2436.
[42] A. Tayyebi, O. Akhavan, B.-K. Lee, M. Outokesh, Carbon 2018, 130, 267.
[43] L. Zdrazil, R. Zahradnicek, R. Mohan, P. Sedlacek, L. Nejdl, V. Schmiedova, J. Pospisil, M. Horak, M. Weiter, O. Zmeskal, Journal of Luminescence 2018, 204, 203.
[44] M. Buzaglo, M. Shtein, O. Regev, Chemistry of Materials 2016, 28, 21.
[45] H. Jin, H. Huang, Y. He, X. Feng, S. Wang, L. Dai, J. Wang, Journal of the American Chemical Society 2015, 137, 7588.
[46] D. Qu, M. Zheng, P. Du, Y. Zhou, L. Zhang, D. Li, H. Tan, Z. Zhao, Z. Xie, Z. Sun, Nanoscale 2013, 5, 12272.
[47] Y. Q. Dong, J. W. Shao, C. Q. Chen, H. Li, R. X. Wang, Y. W. Chi, X. M. Lin, G. N. Chen, Carbon 2012, 50, 4738.
[48] S. Zhu, Q. Meng, L. Wang, J. Zhang, Y. Song, H. Jin, K. Zhang, H. Sun, H. Wang, B. Yang, Angewandte Chemie 2013, 125, 4045; J. Schneider, C. J. Reckmeier, Y. Xiong, M. von Seckendorff, A. S. Susha, P. Kasak, A. L. Rogach, Journal of Physical Chemistry C 2017, 121, 2014; R. Z. Zhang, J. R. Adsetts, Y. T. Nie, X. H. Sun, Z. F. Ding, Carbon 2018, 129, 45.
[49] S. J. Jeon, T. W. Kang, J. M. Ju, M. J. Kim, J. H. Park, F. Raza, J. Han, H. R. Lee, J. H. Kim, Advanced Functional Materials 2016, 26, 8211.
[50] J. Zhu, Y. Tang, G. Wang, J. Mao, Z. Liu, T. Sun, M. Wang, D. Chen, Y. Yang, J. Li, Y. Deng, S. Yang, ACS Applied Materials & Interfaces 2017, 9, 14470.
[51] Z. Wang, J. Yu, X. Zhang, N. Li, B. Liu, Y. Li, Y. Wang, W. Wang, Y. Li, L. Zhang, S. Dissanayake, S. L. Suib, L. Sun, ACS Applied Materials & Interfaces 2016, 8, 1434; A. Abbas, L. T. Mariana, A. N. Phan, Carbon 2018, 140, 77; A. Suryawanshi, M. Biswal, D. Mhamane, R. Gokhale, S. Patil, D. Guin, S. Ogale, Nanoscale 2014, 6, 11664; Z. Ding, F. Li, J. Wen, X. Wang, R. Sun, Green Chemistry 2018, 20, 1383.

[52] A. Ananthanarayanan, Y. Wang, P. Routh, M. A. Sk, A. Than, M. Lin, J. Zhang, J. Chen, H. Sun, P. Chen, Nanoscale 2015, 7, 8159.
[53] T. F. Yeh, W. L. Huang, C. J. Chung, I. T. Chiang, L. C. Chen, H. Y. Chang, W. C. Su, C. Cheng, S. J. Chen, H. S. Teng, Journal of Physical Chemistry Letters 2016, 7, 2087.
[54] R. Ye, Z. Peng, A. Metzger, J. Lin, J. A. Mann, K. Huang, C. Xiang, X. Fan, E. L. G. Samuel, L. B. Alemany, A. A. Martí, J. M. Tour, ACS Applied Materials & Interfaces 2015, 7, 7041.
[55] Z. Gan, H. Xu, Y. Hao, Nanoscale 2016, 8, 7794.
[56] F. Zhang, F. Liu, C. Wang, X. Xin, J. Liu, S. Guo, J. Zhang, ACS Applied Materials & Interfaces 2016, 8, 2104.
[57] L. Li, G. Wu, G. Yang, J. Peng, J. Zhao, J. J. Zhu, Nanoscale 2013, 5, 4015; S. Chen, N. Ullah, T. Wang, R. Zhang, Journal of Materials Chemistry C 2018, 6, 6875.
[58] H. J. Sun, L. Wu, N. Gao, J. S. Ren, X. G. Qu, Acs Applied Materials & Interfaces 2013, 5, 1174; C. F. Hu, Y. L. Liu, Y. H. Yang, J. H. Cui, Z. R. Huang, Y. L. Wang, L. F. Yang, H. B. Wang, Y. Xiao, J. H. Rong, Journal of Materials Chemistry B 2013, 1, 39.
[59] H. Sun, A. Zhao, N. Gao, K. Li, J. Ren, X. Qu, Angewandte Chemie International Edition 2015, 54, 7176.
[60] K. Li, J. Chen, Y. Yan, Y. Min, H. Li, F. Xi, J. Liu, P. Chen, Carbon 2018, 136, 224.
[61] A. Shomali, H. Valizadeh, A. Banan, R. Mohammad-Rezaei, RSC Advances 2015, 5, 88202.
[62] J. Feng, H. Dong, B. Pang, F. Shao, C. Zhang, L. Yu, L. Dong, Physical Chemistry Chemical Physics 2018, 20, 15244.
[63] L. Zhang, D. Peng, R.-P. Liang, J.-D. Qiu, Analytical Chemistry 2015, 87, 10894.
[64] L. Sun, Y. Luo, M. Li, G. Hu, Y. Xu, T. Tang, J. Wen, X. Li, L. Wang, Journal of Colloid and Interface Science 2017, 508, 154.
[65] X. Deng, J. Sun, S. Yang, H. Shen, W. Zhou, J. Lu, G. Ding, Z. Wang, Applied Physics Letters 2015, 107, 241905.
[66] S. Yang, J. Sun, P. He, X. Deng, Z. Wang, C. Hu, G. Ding, X. Xie, Chemistry of Materials 2015, 27, 2004.
[67] Z. W. Cai, F. M. Li, P. Wu, L. J. Ji, H. Zhang, C. X. Cai, D. F. Gervasio, Analytical Chemistry 2015, 87, 11803; S. R. M. Santiago, T. N. Lin, C. H. Chang, Y. A. Wong, C. A. J. Lin, C. T. Yuan, J. L. Shen, Physical Chemistry Chemical Physics 2017, 19, 22395; W. S. Kuo, H. H. Chen, S. Y. Chen, C. Y. Chang, P. C. Chen, Y. I. Hou, Y. T. Shao, H. F. Kao, C. L. Lilian Hsu, Y. C. Chen, S. J. Chen, S. R. Wu, J. Y. Wang, Biomaterials 2017, 120, 185; B. Y. Fang, C. Li, Y. Y. Song, F. Tan, Y. C. Cao, Y. D. Zhao, Biosensors and Bioelectronics 2018, 100, 41; Q. Liu, B. Guo, Z. Rao, B. Zhang, J. R. Gong, Nano Letters 2013, 13, 2436; M. Miah, S. Bhattacharya, A. Gupta, S. K. Saha, Electrochimica Acta 2016, 222, 709.
[68] S. Kundu, R. M. Yadav, T. N. Narayanan, M. V. Shelke, R. Vajtai, P. M. Ajayan, V. K. Pillai, Nanoscale 2015, 7, 11515.
[69] H. L. Fei, R. Q. Ye, G. L. Ye, Y. J. Gong, Z. W. Peng, X. J. Fan, E. L. G. Samuel, P. M. Ajayan, J. M. Tour, Acs Nano 2014, 8, 10837.
[70] Y. Li, S. Li, Y. M. Wang, J. Wang, H. Liu, X. Q. Liu, L. F. Wang, X. G. Liu, W. D. Xue, N. Ma, Physical Chemistry Chemical Physics 2017, 19, 11631.
[71] Q. Feng, Q. Q. Cao, M. Li, F. C. Liu, N. J. Tang, Y. W. Du, Applied Physics Letters 2013, 102, 013111.
[72] J. C. Ge, M. H. Lan, B. J. Zhou, W. M. Liu, L. Guo, H. Wang, Q. Y. Jia, G. L. Niu, X. Huang, H. Y. Zhou, X. M. Meng, P. F. Wang, C. S. Lee, W. J. Zhang, X. D. Han, Nature Communications 2014, 5, 4596.

[73] D. Huang, H. Zhou, Y. Wu, T. Wang, L. Sun, P. Gao, Y. Sun, H. Huang, G. Zhou, J. Hu, Carbon 2019, 142, 673.
[74] M. Yan, Y. Hua, F. Zhu, W. Gu, J. Jiang, H. Shen, W. Shi, Applied Catalysis B: Environmental 2017, 202, 518.
[75] S. Y. Bian, C. Shen, Y. T. Qian, J. Y. Liu, F. N. Xi, X. P. Dong, Sensors and Actuators B-Chemical 2017, 242, 231.
[76] H. M. Kashani, T. Madrakian, A. Afkhami, New Journal of Chemistry 2017, 41, 6875.
[77] Z. L. Wu, M. X. Gao, T. T. Wang, X. Y. Wan, L. L. Zheng, C. Z. Huang, Nanoscale 2014, 6, 3868; T. V. Tam, N. B. Trung, H. R. Kim, J. S. Chung, W. M. Choi, Sensors and Actuators B-Chemical 2014, 202, 568; Z. Liu, J. Xiao, X. Wu, L. Lin, S. Weng, M. Chen, X. Cai, X. Lin, Sensors and Actuators B: Chemical 2016, 229, 217; M. T. Hasan, R. Gonzalez-Rodriguez, C. Ryan, N. Faerber, J. L. Coffer, A. V. Naumov, Advanced Functional Materials 2018, 28, 1804337.
[78] C. Chen, D. Zhao, T. Hu, J. Sun, X. Yang, Sensors and Actuators B: Chemical 2017, 241, 779.
[79] D. Qu, M. Zheng, P. Du, Y. Zhou, L. G. Zhang, D. Li, H. Q. Tan, Z. Zhao, Z. G. Xie, Z. C. Sun, Nanoscale 2013, 5, 12272.
[80] H. Wang, R. Revia, K. Wang, R. J. Kant, Q. X. Mu, Z. Gai, K. L. Hong, M. Q. Zhang, Advanced Materials 2017, 29, 1605416.
[81] G. Wang, Q. Guo, D. Chen, Z. Liu, X. Zheng, A. Xu, S. Yang, G. Ding, ACS Applied Materials & Interfaces 2018, 10, 5750.
[82] J. H. Shen, Y. H. Zhu, X. L. Yang, J. Zong, J. M. Zhang, C. Z. Li, New Journal of Chemistry 2012, 36, 97; L. L. Li, G. H. Wu, G. H. Yang, J. Peng, J. W. Zhao, J. J. Zhu, Nanoscale 2013, 5, 4015.
[83] X. Hai, J. Feng, X. Chen, J. Wang, Journal of Materials Chemistry B 2018, 6, 3219.
[84] H. Tetsuka, A. Nagoya, T. Fukusumi, T. Matsui, Advanced Materials 2016, 28, 4632.
[85] B. P. Qi, H. Hu, L. Bao, Z. L. Zhang, B. Tang, Y. Peng, B. S. Wang, D. W. Pang, Nanoscale 2015, 7, 5969.
[86] Y. Yan, J. Chen, N. Li, J. Tian, K. Li, J. Jiang, J. Liu, Q. Tian, P. Chen, ACS Nano 2018, 12, 3523.
[87] P. Gao, K. Ding, Y. Wang, K. Q. Ruan, S. L. Diao, Q. Zhang, B. Q. Sun, J. S. Jie, Journal of Physical Chemistry C 2014, 118, 5164.
[88] S. L. Diao, X. J. Zhang, Z. B. Shao, K. Ding, J. S. Jie, X. H. Zhang, Nano Energy 2017, 31, 359.
[89] K. D. Lee, M. J. Park, D.-Y. Kim, S. M. Kim, B. Kang, S. Kim, H. Kim, H.-S. Lee, Y. Kang, S. S. Yoon, B. H. Hong, D. Kim, ACS Applied Materials & Interfaces 2015, 7, 19043.
[90] M. L. Tsai, D. S. Tsai, L. Tang, L. J. Chen, S. P. Lau, J. H. He, ACS Nano 2017, 11, 4564.
[91] J. K. Kim, M. J. Park, S. J. Kim, D. H. Wang, S. P. Cho, S. Bae, J. H. Park, B. H. Hong, ACS Nano 2013, 7, 7207.
[92] M. L. Tsai, W. R. Wei, L. Tang, H. C. Chang, S. H. Tai, P. K. Yang, S. P. Lau, L. J. Chen, J. H. He, ACS Nano 2016, 10, 815; B. J. Moon, D. Jang, Y. Yi, H. Lee, S. J. Kim, Y. Oh, S. H. Lee, M. Park, S. Lee, S. Bae, Nano Energy 2017, 34, 36.
[93] M. L. Tsai, W. C. Tu, L. Tang, T. C. Wei, W. R. Wei, S. P. Lau, L. J. Chen, J. H. He, Nano Letters 2016, 16, 309.
[94] Z. Ding, Z. Hao, B. Meng, Z. Xie, J. Liu, L. Dai, Nano Energy 2015, 15, 186.
[95] J. Ryu, J. W. Lee, H. Yu, J. Yun, K. Lee, J. Lee, D. Hwang, J. Kang, S. K. Kim, J. Jang, Journal of Materials Chemistry A 2017, 5, 16834; Z. L. Zhu, J. A. Ma, Z. L. Wang, C. Mu, Z. T. Fan, L. L. Du, Y. Bai, L. Z. Fan, H. Yan, D. L. Phillips, S. H. Yang, Journal of the American Chemical Society 2014, 136, 3760; Z. Yang, J. Xie, V. Arivazhagan, K. Xiao, Y. Qiang, K. Huang, M. Hu, C. Cui, X. Yu, D. Yang, Nano Energy 2017, 40, 345; Z. Ding, Z. Miao, Z. Xie, J. Liu, Journal of Materials Chemistry A

2016, 4, 2413; H. C. Lim, S. H. Min, E. Lee, J. Jang, S. H. Kim, J.-I. Hong, ACS Applied Materials & Interfaces 2015, 7, 11069; C.-P. Lee, K.-Y. Lai, C.-A. Lin, C.-T. Li, K.-C. Ho, C.-I. Wu, S.-P. Lau, J.-H. He, Nano Energy 2017, 36, 260.
[96] S. Kundu, P. Sarojinijeeva, R. Karthick, G. Anantharaj, G. Saritha, R. Bera, S. Anandan, A. Patra, P. Ragupathy, M. Selvaraj, D. Jeyakumar, K. V. Pillai, Electrochimica Acta 2017, 242, 337.
[97] I. Mihalache, A. Radoi, M. Mihaila, C. Munteanu, A. Marin, M. Danila, M. Kusko, C. Kusko, Electrochimica Acta 2015, 153, 306.
[98] T. G. Novak, J. Kim, S. H. Song, G. H. Jun, H. Kim, M. S. Jeong, S. Jeon, Small 2016, 12, 994.
[99] F. Khan, J. H. Kim, ACS Photonics 2018, 5, 4637.
[100] R. Sekiya, Y. Uemura, H. Murakami, T. Haino, Angewandte Chemie-International Edition 2014, 53, 5619; D. Pan, L. Wang, Z. Li, B. Geng, C. Zhang, J. Zhan, L. Yin, L. Wang, New Journal of Chemistry 2018, 42, 5083; D. H. Kim, T. W. Kim, Nano Energy 2018, 51, 199.
[101] S. H. Song, M. H. Jang, J. Chung, S. H. Jin, B. H. Kim, S. H. Hur, S. Yoo, Y. H. Cho, S. Jeon, Advanced Optical Materials 2014, 2, 1016.
[102] D. H. Kim, T. W. Kim, Nano Energy 2017, 32, 441.
[103] L. B. Tang, R. B. Ji, X. K. Cao, J. Y. Lin, H. X. Jiang, X. M. Li, K. S. Teng, C. M. Luk, S. J. Zeng, J. H. Hao, S. P. Lau, Acs Nano 2012, 6, 5102.
[104] H. Tetsuka, A. Nagoya, R. Asahi, Journal of Materials Chemistry C 2015, 3, 3536.
[105] I. Mihalache, A. Radoi, R. Pascu, C. Romanitan, E. Vasile, M. Kusko, Acs Applied Materials & Interfaces 2017, 9, 29234.
[106] D. A. Nguyen, H. M. Oh, N. T. Duong, S. Bang, S. J. Yoon, M. Seok Jeong, Acs Applied Materials & Interfaces 2018, 10, 10322.
[107] Q. Zhang, J. Jie, S. Diao, Z. Shao, Q. Zhang, L. Wang, W. Deng, W. Hu, H. Xia, X. Yuan, S.-T. Lee, ACS Nano 2015, 9, 1561.
[108] D. Ghosh, S. Kapri, S. Bhattacharyya, Acs Applied Materials & Interfaces 2016, 8, 35496.
[109] S. Dhar, T. Majumder, S. P. Mondal, Acs Applied Materials & Interfaces 2016, 8, 31822.
[110] G. Haider, P. Roy, C. W. Chiang, W. C. Tan, Y. R. Liou, H. T. Chang, C. T. Liang, W. H. Shih, Y. F. Chen, Advanced Functional Materials 2016, 26, 620.
[111] H. Tetsuka, A. Nagoya, S.-i. Tamura, Nanoscale 2016, 8, 19677.
[112] S. K. Lai, C. M. Luk, L. B. Tang, K. S. Teng, S. P. Lau, Nanoscale 2015, 7, 5338.
[113] S. Li, T. Fan, X. Liu, F. Liu, H. Meng, Y. Liu, F. Pan, ACS Applied Materials & Interfaces 2017, 9, 3677.
[114] Y. T. Liang, C. G. Lu, D. F. Ding, M. Zhao, D. W. Wang, C. Hu, J. S. Qiu, G. Xie, Z. Y. Tang, Chemical Science 2015, 6, 4103.
[115] Y. Hu, Y. Zhao, G. Lu, N. Chen, Z. Zhang, H. Li, H. Shao, L. Qu, Nanotechnology 2013, 24, 195401.
[116] H. Jia, Y. Cai, J. Lin, H. Liang, J. Qi, J. Cao, J. Feng, W. Fei, Advanced Science 2018, 5, 1700887.
[117] Y. Liu, R. Wang, J. Lang, X. Yan, Physical Chemistry Chemical Physics 2015, 17, 14028.
[118] W.-W. Liu, Y.-Q. Feng, X.-B. Yan, J.-T. Chen, Q.-J. Xue, Advanced Functional Materials 2013, 23, 4111; M. Hassan, E. Haque, K. R. Reddy, A. I. Minett, J. Chen, V. G. Gomes, Nanoscale 2014, 6, 11988.
[119] A. B. Ganganboina, A. D. Chowdhury, R.-a. Doong, Electrochimica Acta 2017, 245, 912.
[120] Z. Li, L. Cao, P. Qin, X. Liu, Z. Chen, L. Wang, D. Pan, M. Wu, Carbon 2018, 139, 67; Z. Li, X. Liu, L. Wang, F. Bu, J. Wei, D. Pan, M. Wu, Small 2018, 14, 1801498.
[121] M. Miah, S. Bhattacharya, A. Gupta, S. K. Saha, Electrochimica Acta 2016, 222, 709.

[122] Z. Li, P. Qin, L. Wang, C. Yang, Y. Li, Z. Chen, D. Pan, M. Wu, Electrochimica Acta 2016, 208, 260.
[123] Q. Chen, Y. Hu, C. Hu, H. Cheng, Z. Zhang, H. Shao, L. Qu, Physical Chemistry Chemical Physics 2014, 16, 19307.
[124] K. Lee, H. Lee, Y. Shin, Y. Yoon, D. Kim, H. Lee, Nano Energy 2016, 26, 746.
[125] S. Mondal, U. Rana, S. Malik, Chemical Communications 2015, 51, 12365.
[126] J. Guo, H. Zhu, Y. Sun, L. Tang, X. Zhang, Journal of Materials Chemistry A 2016, 4, 4783.
[127] Y. M. Chen, S. T. Hsu, Y. H. Tseng, T. F. Yeh, S. S. Hou, J. S. Jan, Y. L. Lee, H. Teng, Small 2018, 14, 1703571.
[128] J. Park, J. Moon, C. Kim, J. H. Kang, E. Lim, J. Park, K. J. Lee, S.-H. Yu, J.-H. Seo, J. Lee, J. Heo, N. Tanaka, S.-P. Cho, J. Pyun, J. Cabana, B. H. Hong, Y.-E. Sung, Npg Asia Materials 2016, 8, e272.
[129] K. Lijuan, Y. Yongqiang, L. Ruiyi, L. Zaijun, Electrochimica Acta 2016, 198, 144.
[130] L. Ruiyi, J. Yuanyuan, Z. Xiaoyan, L. Zaijun, G. Zhiguo, W. Guangli, L. Junkang, Electrochimica Acta 2015, 178, 303.
[131] D. Chao, C. Zhu, X. Xia, J. Liu, X. Zhang, J. Wang, P. Liang, J. Lin, H. Zhang, Z. X. Shen, H. J. Fan, Nano Letters 2015, 15, 565.
[132] C. Zhu, D. Chao, J. Sun, I. M. Bacho, Z. Fan, C. F. Ng, X. Xia, H. Huang, H. Zhang, Z. X. Shen, G. Ding, H. J. Fan, Advanced Materials Interfaces 2015, 2, 1400499.
[133] Y. Ji, J. Hu, J. Biskupek, U. Kaiser, Y. F. Song, C. Streb, Chemistry – A European Journal 2017, 23, 16637.
[134] S. Yu, Y.-Q. Zhong, B.-Q. Yu, S.-Y. Cai, L.-Z. Wu, Y. Zhou, Physical Chemistry Chemical Physics 2016, 18, 20338.
[135] M. Yan, Y. Hua, F. Zhu, L. Sun, W. Gu, W. Shi, Applied Catalysis B: Environmental 2017, 206, 531.
[136] Y. Lei, C. Yang, J. Hou, F. Wang, S. Min, X. Ma, Z. Jin, J. Xu, G. Lu, K.-W. Huang, Applied Catalysis B: Environmental 2017, 216, 59.
[137] J. Gliniak, J. H. Lin, Y. T. Chen, C. R. Li, E. Jokar, C. H. Chang, C. S. Peng, J. N. Lin, W. H. Lien, H. M. Tsai, T. K. Wu, ChemSusChem 2017, 10, 3260.
[138] D. Qu, Z. Sun, M. Zheng, J. Li, Y. Zhang, G. Zhang, H. Zhao, X. Liu, Z. Xie, Advanced Optical Materials 2015, 3, 360.
[139] D. Yadav, R. K. Yadav, A. Kumar, N. J. Park, J. O. Baeg, ChemCatChem 2016, 8, 3389.
[140] J. Hou, S. Cao, Y. Wu, F. Liang, L. Ye, Z. Lin, L. Sun, Nano Energy 2016, 30, 59.
[141] Q. Lu, Y. Zhang, S. Liu, Journal of Materials Chemistry A 2015, 3, 8552.
[142] S. Bian, C. Zhou, P. Li, J. Liu, X. Dong, F. Xi, ChemCatChem 2017, 9, 3349; D. Pan, J. Jiao, Z. Li, Y. Guo, C. Feng, Y. Liu, L. Wang, M. Wu, ACS Sustainable Chemistry & Engineering 2015, 3, 2405.
[143] M. Ebrahimi, M. Samadi, S. Yousefzadeh, M. Soltani, A. Rahimi, T.-c. Chou, L.-C. Chen, K.-H. Chen, A. Z. Moshfegh, ACS Sustainable Chemistry & Engineering 2017, 5, 367.
[144] Y. Hao, X. Dong, X. Wang, S. Zhai, H. Ma, X. Zhang, Journal of Materials Chemistry A 2016, 4, 8298.
[145] J. Liu, H. Xu, Y. Xu, Y. Song, J. Lian, Y. Zhao, L. Wang, L. Huang, H. Ji, H. Li, Applied Catalysis B: Environmental 2017, 207, 429.
[146] J. Qian, C. Shen, J. Yan, F. Xi, X. Dong, J. Liu, The Journal of Physical Chemistry C 2018, 122, 349.
[147] M. Mahyari, Y. Bide, J. N. Gavgani, Applied Catalysis A: General 2016, 517, 100.

[148] Y. Liu, S. Yu, Z. Zhao, F. Dong, X. A. Dong, Y. Zhou, The Journal of Physical Chemistry C 2017, 121, 12168.
[149] C. Xu, Q. Han, Y. Zhao, L. Wang, Y. Li, L. Qu, Journal of Materials Chemistry A 2015, 3, 1841.
[150] X. Zhou, Z. Tian, J. Li, H. Ruan, Y. Ma, Z. Yang, Y. Qu, Nanoscale 2014, 6, 2603.
[151] M. Fan, C. Zhu, J. Yang, D. Sun, Electrochimica Acta 2016, 216, 102.
[152] H. Fei, R. Ye, G. Ye, Y. Gong, Z. Peng, X. Fan, E. L. G. Samuel, P. M. Ajayan, J. M. Tour, ACS Nano 2014, 8, 10837.
[153] M. Favaro, L. Ferrighi, G. Fazio, L. Colazzo, C. Di Valentin, C. Durante, F. Sedona, A. Gennaro, S. Agnoli, G. Granozzi, ACS Catalysis 2015, 5, 129.
[154] Y. Liu, P. Wu, ACS Applied Materials & Interfaces 2013, 5, 3362.
[155] B. Zhang, C. Xiao, Y. Xiang, B. Dong, S. Ding, Y. Tang, ChemElectroChem 2016, 3, 864; T. Van Tam, S. G. Kang, K. F. Babu, E.-S. Oh, S. G. Lee, W. M. Choi, Journal of Materials Chemistry A 2017, 5, 10537.
[156] R. Vinoth, I. M. Patil, A. Pandikumar, B. A. Kakade, N. M. Huang, D. D. Dionysios, B. Neppolian, ACS Omega 2016, 1, 971.
[157] J. Q. Tian, J. Chen, J. Y. Liu, Q. H. Tian, P. Chen, Nano Energy 2018, 48, 284.
[158] J. J. Lv, J. Zhao, H. Fang, L. P. Jiang, L. L. Li, J. Ma, J. J. Zhu, Small 2017, 13.
[159] A. Muthurasu, S. V. S. Mers, V. Ganesh, International Journal of Hydrogen Energy 2018, 43, 4726.
[160] S. Kundu, B. Malik, D. K. Pattanayak, P. Ragupathy, V. K. Pillai, Chemistryselect 2017, 2, 9943.
[161] J. Guo, H. Zhu, Y. Sun, L. Tang, X. Zhang, Electrochimica Acta 2016, 211, 603.
[162] J. J. Lv, J. Zhao, H. Fang, L. P. Jiang, L. L. Li, J. Ma, J. J. Zhu, Small 2017, 13, 1700264.
[163] X. Wang, W. Yuan, Y. Yu, C. M. Li, ChemSusChem 2017, 10, 1014.
[164] J. Wu, S. Ma, J. Sun, J. I. Gold, C. Tiwary, B. Kim, L. Zhu, N. Chopra, I. N. Odeh, R. Vajtai, Nature communications 2016, 7, 13869.
[165] X. Zou, M. Liu, J. Wu, P. M. Ajayan, J. Li, B. Liu, B. I. Yakobson, ACS Catalysis 2017, 7, 6245.
[166] X. Qiao, Q. Li, R. N. Schaugaard, B. W. Noffke, Y. Liu, D. Li, L. Liu, K. Raghavachari, L.-s. Li, Journal of the American Chemical Society 2017, 139, 3934.
[167] Z. Chen, K. Mou, X. Wang, L. Liu, Angewandte Chemie International Edition 2018, 57, 12790.
[168] Z. Zeng, F. X. Xiao, H. Phan, S. Chen, Z. Yu, R. Wang, T. Q. Nguyen, T. T. Yang Tan, Journal of Materials Chemistry A 2018, 6, 1700.
[169] C. X. Guo, Y. Dong, H. B. Yang, C. M. Li, Advanced Energy Materials 2013, 3, 997.
[170] Z. Zeng, F. X. Xiao, X. Gui, R. Wang, B. Liu, T. T. Yang Tan, Journal of Materials Chemistry A 2016, 4, 16383; H. Li, J. Xing, Z. Xia, J. Chen, Carbon 2015, 81, 474; Z. Zeng, Y. B. Li, S. Chen, P. Chen, F. X. Xiao, J Mater Chem A 2018, 6, 11154.
[171] K. Y. Yoon, H. J. Ahn, M. J. Kwak, P. Thiyagarajan, J. H. Jang, Advanced Optical Materials 2015, 3, 907.
[172] Z. Xu, M. Yin, J. Sun, G. Ding, L. Lu, P. Chang, X. Chen, D. Li, Nanotechnology 2016, 27, 115401.
[173] X. Wu, S. Guo, J. Zhang, Chemical Communications 2015, 51, 6318.
[174] J. Soong Sin, K. Jungkil, K. Soo Seok, K. Sung, C. Suk-Ho, H. Sung Won, Nanotechnology 2014, 25, 255203.

[175] J. Yongsung, K. Juhan, C. An-Na, A. L. Sang, L. Myung Woo, S. Jung Sang, B. Sukang, M. Byung Joon, L. Sang Hyun, L. Dong Su, W. Gunuk, K. Tae-Wook, Nanotechnology 2016, 27, 145204.
[176] Y. H. Kim, E. Y. Lee, H. H. Lee, T. S. Seo, ACS Applied Materials & Interfaces 2017, 9, 16375.
[177] X. Pan, E. Skafidas, Nanoscale 2016, 8, 20074; X. Yan, L. Zhang, H. Chen, X. Li, J. Wang, Q. Liu, C. Lu, J. Chen, H. Wu, P. Zhou, Advanced Functional Materials 2018, 28, 1803728.
[178] E. Hwang, S. Seo, S. Bak, H. Lee, M. Min, H. Lee, Advanced Materials 2014, 26, 5129.
[179] X. T. Zheng, A. Than, A. Ananthanaraya, D.-H. Kim, P. Chen, ACS Nano 2013, 7, 6278.
[180] J. Chen, A. Than, N. Li, A. Ananthanarayanan, X. Zheng, F. Xi, J. Liu, J. Tian, P. Chen, FlatChem 2017, 5, 25.
[181] N. Li, A. Than, C. Sun, J. Tian, J. Chen, K. Pu, X. Dong, P. Chen, ACS Nano 2016, 10, 11475.
[182] N. Li, A. Than, J. Chen, F. N. Xi, J. Y. Liu, P. Chen, Biomaterials Science 2018, 6, 779.
[183] M. K. Kumawat, M. Thakur, R. B. Gurung, R. Srivastava, ACS Sustainable Chemistry & Engineering 2017, 5, 1382.
[184] J. Sun, Q. Xin, Y. Yang, H. Shah, H. Cao, Y. Qi, J. R. Gong, J. Li, Chemical Communications 2018, 54, 715.
[185] W. Zhao, Y. Li, S. Yang, Y. Chen, J. Zheng, C. Liu, Z. Qing, J. Li, R. Yang, Analytical chemistry 2016, 88, 4833.
[186] B. Sapkota, A. Benabbas, H.-Y. G. Lin, W. Liang, P. Champion, M. Wanunu, ACS Applied Materials & Interfaces 2017, 9, 9378.
[187] S. J. Zhu, J. H. Zhang, S. J. Tang, C. Y. Qiao, L. Wang, H. Y. Wang, X. Liu, B. Li, Y. F. Li, W. L. Yu, X. F. Wang, H. C. Sun, B. Yang, Advanced Functional Materials 2012, 22, 4732.
[188] A. Ananthanarayanan, X. Wang, P. Routh, B. Sana, S. Lim, D.-H. Kim, K.-H. Lim, J. Li, P. Chen, Advanced Functional Materials 2014, 24, 3021.
[189] N. Li, A. Than, X. W. Wang, S. H. Xu, L. Sun, H. W. Duan, C. J. Xu, P. Chen, Acs Nano 2016, 10, 3622.
[190] H. Chen, Z. Wang, S. Zong, P. Chen, D. Zhu, L. Wu, Y. Cui, Nanoscale 2015, 7, 15477; X. Su, C. Chan, J. Shi, M.-K. Tsang, Y. Pan, C. Cheng, O. Gerile, M. Yang, Biosensors and Bioelectronics 2017, 92, 489.
[191] J. Zhao, L. Zhao, C. Lan, S. Zhao, Sensors and Actuators B: Chemical 2016, 223, 246.
[192] R. Wang, X. Du, Y. Wu, J. Zhai, X. Xie, ACS sensors 2018.
[193] R. Gao, Z. Zhong, X. Gao, L. Jia, Journal of Agricultural and Food Chemistry 2018, 66, 10898.
[194] M. Roushani, S. Kohzadi, S. Haghjoo, A. Azadbakht, Environmental Nanotechnology, Monitoring & Management 2018, 10, 308.
[195] Z. Li, Y. Wang, Y. Ni, S. Kokot, Sensors and Actuators B: Chemical 2015, 207, 490.
[196] H. Huang, Z. Feng, Y. Li, Z. Liu, L. Zhang, Y. Ma, J. Tong, Analytical Methods 2015, 7, 2928.
[197] F. Nemati, M. Hosseini, R. Zare-Dorabei, M. R. Ganjali, Analytical Methods 2018, 10, 1760.
[198] Y. M. Chen, Y. Q. Dong, H. Wu, C. Q. Chen, Y. W. Chi, G. N. Chen, Electrochimica Acta 2015, 151, 552; G. Nie, Y. Wang, Y. Tang, D. Zhao, Q. Guo, Biosensors and Bioelectronics 2018, 101, 123; Y. Yang, G. Fang, X. Wang, F. Zhang, J. Liu, W. Zheng, S. Wang, Electrochimica Acta 2017, 228, 107.
[199] F. Zuo, C. Zhang, H. Zhang, X. Tan, S. Chen, R. Yuan, Electrochimica Acta 2019, 294, 76.
[200] J. Lou, S. Liu, W. Tu, Z. Dai, Analytical Chemistry 2015, 87, 1145.
[201] P. Zhang, Y. Zhuo, Y. Chang, R. Yuan, Y. Chai, Analytical Chemistry 2015, 87, 10385.

[202] Y. Dong, R. Dai, T. Dong, Y. Chi, G. Chen, Nanoscale 2014, 6, 11240.
[203] H. Chen, W. Li, Q. Wang, X. Jin, Z. Nie, S. Yao, Electrochimica Acta 2016, 214, 94.
[204] S. L. Ting, S. J. Ee, A. Ananthanarayanan, K. C. Leong, P. Chen, Electrochimica Acta 2015, 172, 7; T.-T. Xu, J.-X. Yang, J.-M. Song, J.-S. Chen, H.-L. Niu, C.-J. Mao, S.-Y. Zhang, Y.-H. Shen, Sensors and Actuators B: Chemical 2017, 243, 863.
[205] L. Lu, L. Zhou, J. Chen, F. Yan, J. Liu, X. Dong, F. Xi, P. Chen, ACS Nano 2018, DOI: 10.1021/acsnano.8b07564.
[206] P. Pang, F. Yan, H. Li, H. Li, Y. Zhang, H. Wang, Z. Wu, W. Yang, Analytical Methods 2016, 8, 4912.
[207] S. Baluta, A. Lesiak, J. Cabaj, Electroanalysis 2018, 30, 1781.
[208] T. Zhang, Y. Gu, C. Li, X. Yan, N. Lu, H. Liu, Z. Zhang, H. Zhang, ACS Applied Materials & Interfaces 2017, 9, 37991; J. Xi, C. Xie, Y. Zhang, L. Wang, J. Xiao, X. Duan, J. Ren, F. Xiao, S. Wang, ACS Applied Materials & Interfaces 2016, 8, 22563.
[209] J. Liu, D. Tang, Z. Chen, X. Yan, Z. Zhong, L. Kang, J. Yao, Biosensors and Bioelectronics 2017, 94, 271.
[210] L.-L. Feng, Y.-X. Wu, D.-L. Zhang, X.-X. Hu, J. Zhang, P. Wang, Z.-L. Song, X.-B. Zhang, W. Tan, Analytical Chemistry 2017, 89, 4077.
[211] E. Zor, E. Morales-Narváez, A. Zamora-Gálvez, H. Bingol, M. Ersoz, A. Merkoçi, ACS Applied Materials & Interfaces 2015, 7, 20272.
[212] N. Li, X. Wang, J. Chen, L. Sun, P. Chen, 2D Materials 2015, 2, 034018.
[213] Y. Yan, Q. Liu, X. Du, J. Qian, H. Mao, K. Wang, Analytica Chimica Acta 2015, 853, 258.
[214] Y. Zang, J. Lei, Q. Hao, H. Ju, ACS applied materials & interfaces 2014, 6, 15991.
[215] H. Wang, B. Zhang, F. Zhao, B. Zeng, ACS applied materials & interfaces 2018, 10, 35281.
[216] Y. Xianxian, N. Xingxing, M. Kexin, H. Ping, G. Julia, K. Stefan, Z. Yufang, Small 2017, 13, 1602225.
[217] Y. Xuan, R.-Y. Zhang, X.-S. Zhang, J. An, K. Cheng, C. Li, X.-L. Hou, Y.-D. Zhao, Nanotechnology 2018, 29, 355101.
[218] S. Li, S. Zhou, Y. Li, X. Li, J. Zhu, L. Fan, S. Yang, ACS Applied Materials & Interfaces 2017, 9, 22332.
[219] D. Du, K. Wang, Y. Wen, Y. Li, Y. Y. Li, ACS Applied Materials & Interfaces 2016, 8, 3287.
[220] B. Z. Ristic, M. M. Milenkovic, I. R. Dakic, B. M. Todorovic-Markovic, M. S. Milosavljevic, M. D. Budimir, V. G. Paunovic, M. D. Dramicanin, Z. M. Markovic, V. S. Trajkovic, Biomaterials 2014, 35, 4428.
[221] T. A. Tabish, C. J. Scotton, D. C. J Ferguson, L. Lin, A. v. der Veen, S. Lowry, M. Ali, F. Jabeen, M. Ali, P. G. Winyard, Nanomedicine 2018, 13, 1923; W. S. Kuo, Y. T. Shao, C. H. Yang, K. S. Huang, M. H. Hsieh, P. C. Chen, C. Y. Chang, C. H. Huang, C. L. L. Hsu, T. M. Chou, J. Y. Wang, P. C. Wu, ACS Applied Materials & Interfaces 2018, 10, 14438.
[222] W.-S. Kuo, C.-Y. Chang, H.-H. Chen, C.-L. L. Hsu, J.-Y. Wang, H.-F. Kao, L. C.-S. Chou, Y.-C. Chen, S.-J. Chen, W.-T. Chang, ACS applied materials & interfaces 2016, 8, 30467.
[223] W.-S. Kuo, H.-H. Chen, S.-Y. Chen, C.-Y. Chang, P.-C. Chen, Y.-I. Hou, Y.-T. Shao, H.-F. Kao, C.-L. L. Hsu, Y.-C. Chen, Biomaterials 2017, 120, 185.
[224] D. Iannazzo, A. Pistone, S. Ferro, L. De Luca, A. M. Monforte, R. Romeo, M. R. Buemi, C. Pannecouque, Bioconjugate Chemistry 2018, 29, 3084.
[225] D. Kim, J. M. Yoo, H. Hwang, J. Lee, S. H. Lee, S. P. Yun, M. J. Park, M. Lee, S. Choi, S. H. Kwon, S. Lee, S.-H. Kwon, S. Kim, Y. J. Park, M. Kinoshita, Y.-H. Lee, S. Shin, S. R. Paik, S. J. Lee, S. Lee, B. H. Hong, H. S. Ko, Nature Nanotechnology 2018, 13, 812.

[226] M. Wang, Y. Sun, X. Cao, G. Peng, I. Javed, A. Kakinen, T. P. Davis, S. Lin, J. Liu, F. Ding, P. C. Ke, Nanoscale 2018, 10, 19995.
[227] N. Suzuki, Y. Wang, P. Elvati, Z.-B. Qu, K. Kim, S. Jiang, E. Baumeister, J. Lee, B. Yeom, J. H. Bahng, ACS nano 2016, 10, 1744.
[228] G. S. Kumar, U. Thupakula, P. K. Sarkar, S. Acharya, RSC Advances 2015, 5, 27711.

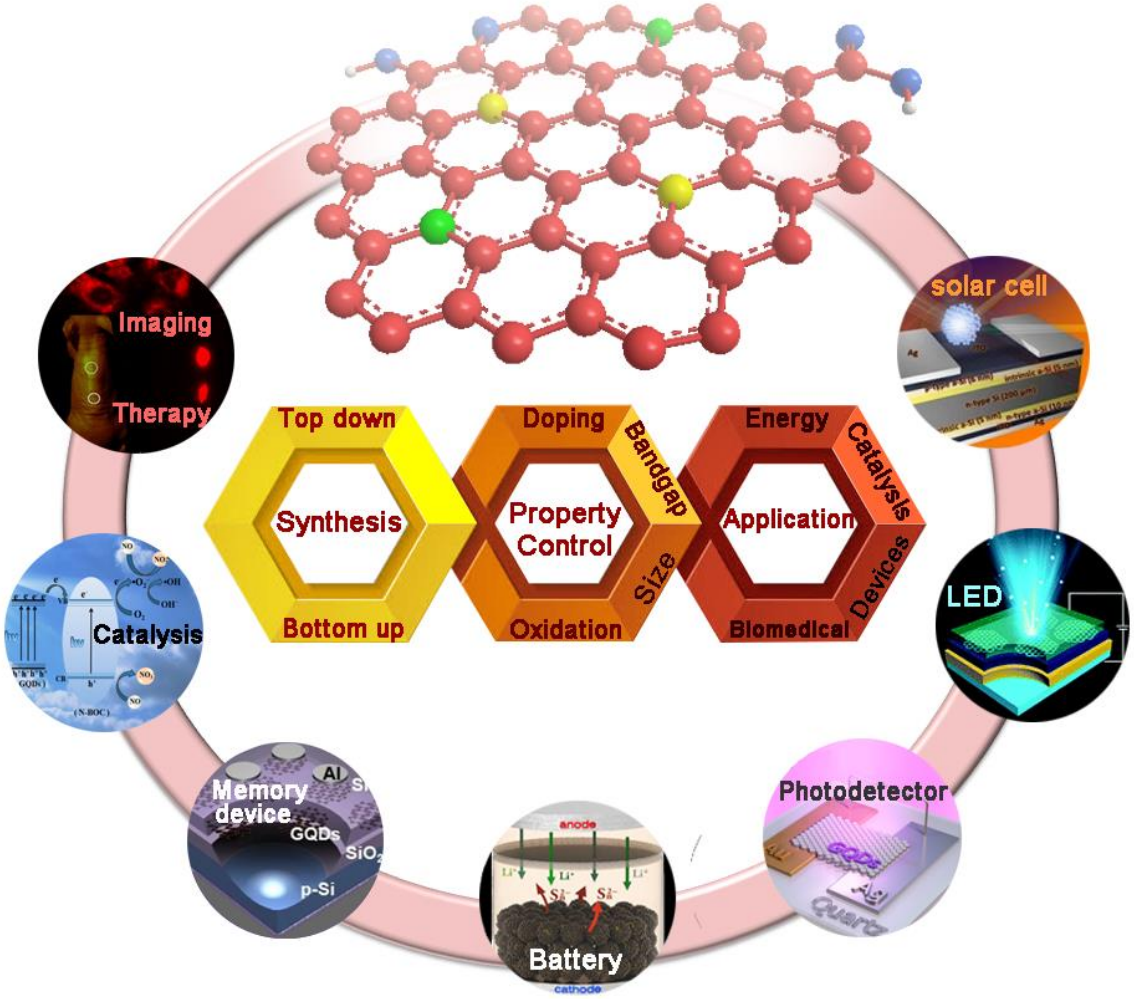

Figure 1 Illustration of the overview of GQD research (main topics of this article). Images from ref. [93], [228], [107], [128], [174], [148] and [72] are used with persimission by American Chemical Society © 2015, 2016, Royal Society of Chemistry © 2015, Springer Nature © 2014, 2016, IOP publishing © 2014.

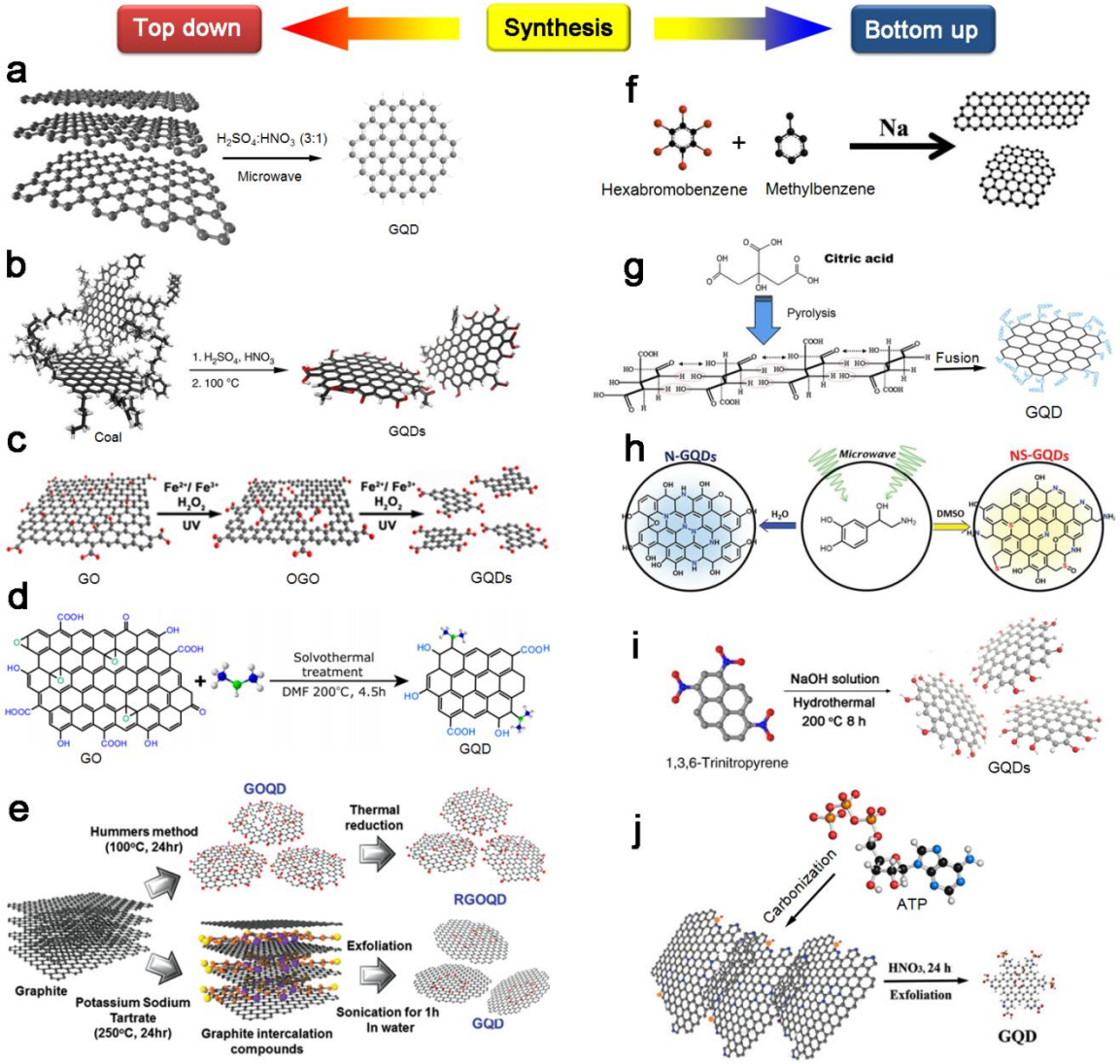

Figure 2 Top-down and bottom-up synthesis of GQDs. (a-c) Top-down oxidative cutting of graphite (a) permitted by John Wiley & Sons © 2016,[8] coal (b) permitted by Springer Nature © 2013,[28] and GO (c) permitted by American Chemical Society © 2012.[31] (d) Reductive cutting of GO permitted by American Chemical Society © 2013.[41] (e) Hummers method (oxidative cutting) and physical exfoliation to prepare GQDs, with permission from John Wiley and Sons © 2016.[10] (f-j) Bottom up synthesis of GQDs from hexabromobenzene and methylbenzene (f) permitted by American Chemical Society © 2015,[45] citric acid (g) permitted by Elsevier © 2012,[47] norepinephrine (h) permitted by John Wiley & Sons © 2016,[49] 1,3,6-trinitropyrene (i) permitted by Springer Nature © 2014,[14] and ATP (j) permitted by Royal Society of Chemistry © 2015.[52]

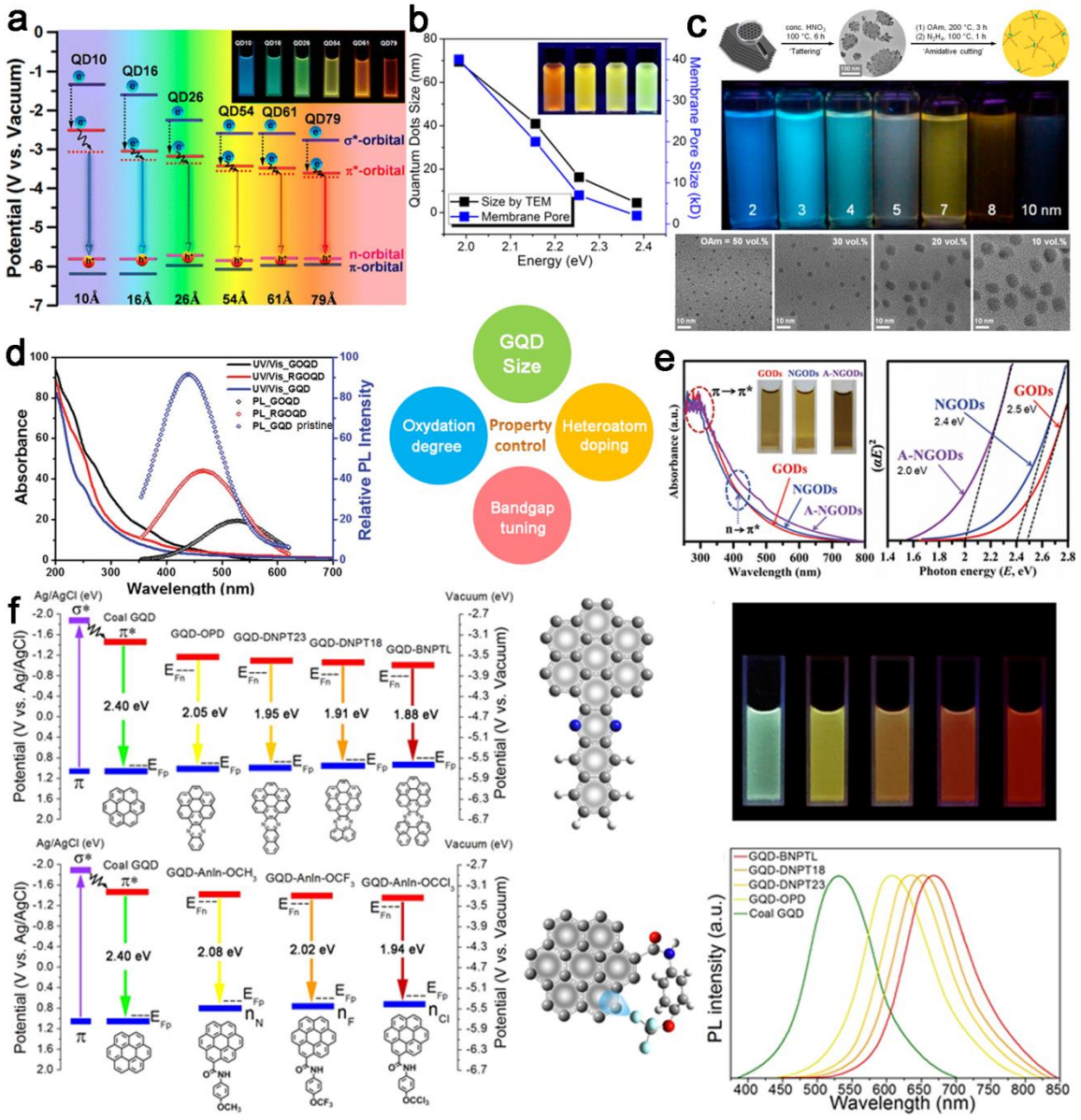

Figure 3 Control of GQD properties. (a) GQDs sieved by membranes with different pore-sizes manifest different bandgap structures,[53] permitted by American Chemical Society © 2016. (b) Bandgap increases with the reducing size of GQDs obtained via longer cutting time and higher reaction temperature,[54] permitted by American Chemical Society © 2015. (c) Bandgap narrows with the increasing size of GQDs obtained from decreasing concentration of cutting agents,[38] permitted by American Chemical Society © 2014. (d) PL redshift and enhanced light adsorption with increasing oxygen content,[10] permitted by John Wiley & Sons © 2016. (e) Light absorption increases with narrowing

bandgap induced by increasing the amount of nitrogen dopant,[25] permitted by John Wiley & Sons © 2016. (f) Bandgap narrowing by enlarging π-conjugated system or grafting electron-donating chemical groups. Reprinted with permission by American Chemical Society © 2018.[86]

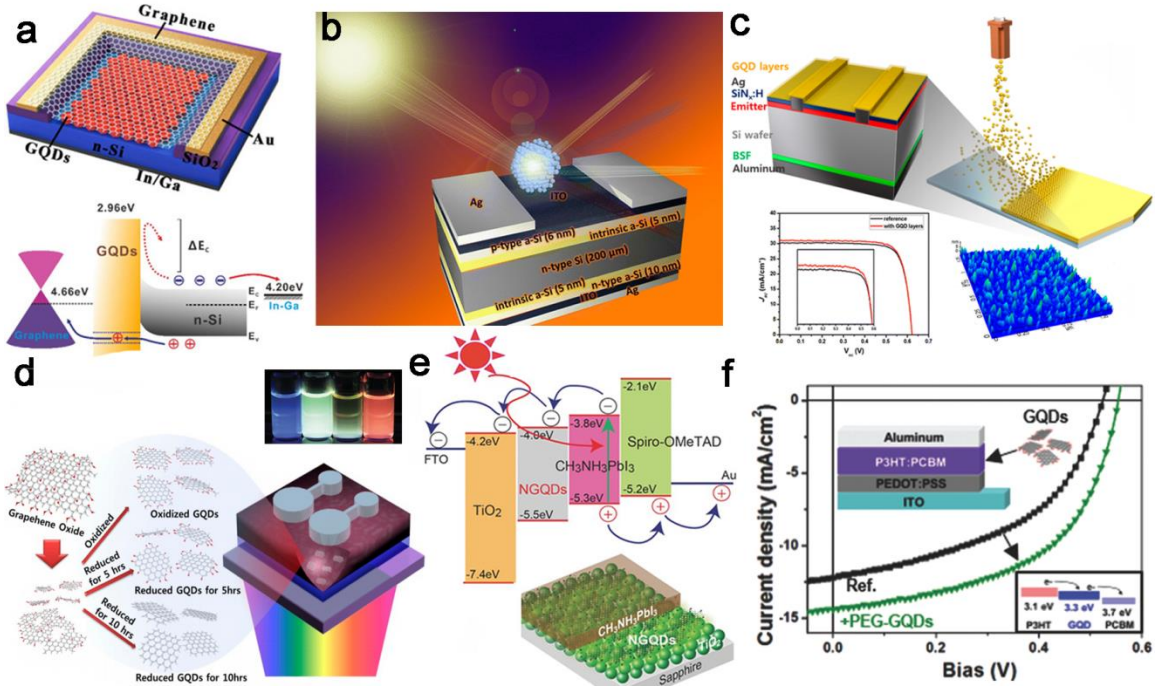

Figure 4 GQDs for photovoltaic devices. (a) GQD/Si heterojunction solar cell with graphene film as the transparent electrode and its energy band diagram,[88] permitted by Elsevier © 2017. (b) Structure of GQD/Si heterojunction solar cell using GQDs as the down-conversion light absorption layer,[93] permitted by American Chemical Society © 2016. (c) GQDs as the light absorption layer on Si solar cell,[89] permitted by American Chemical Society © 2015. (d) GQDs as charge carrier extraction layer in a solar cell,[91] permitted by American Chemical Society © 2013. (e) Energy band structure of the perovskite solar cell using GQDs with different bandgaps,[84] permitted by John Wiley & Sons © 2016. (f) GQDs favors light absorption and exciton dissociation in dye sensitized solar cell,[98] permitted by John Wiley & Sons ©2016.

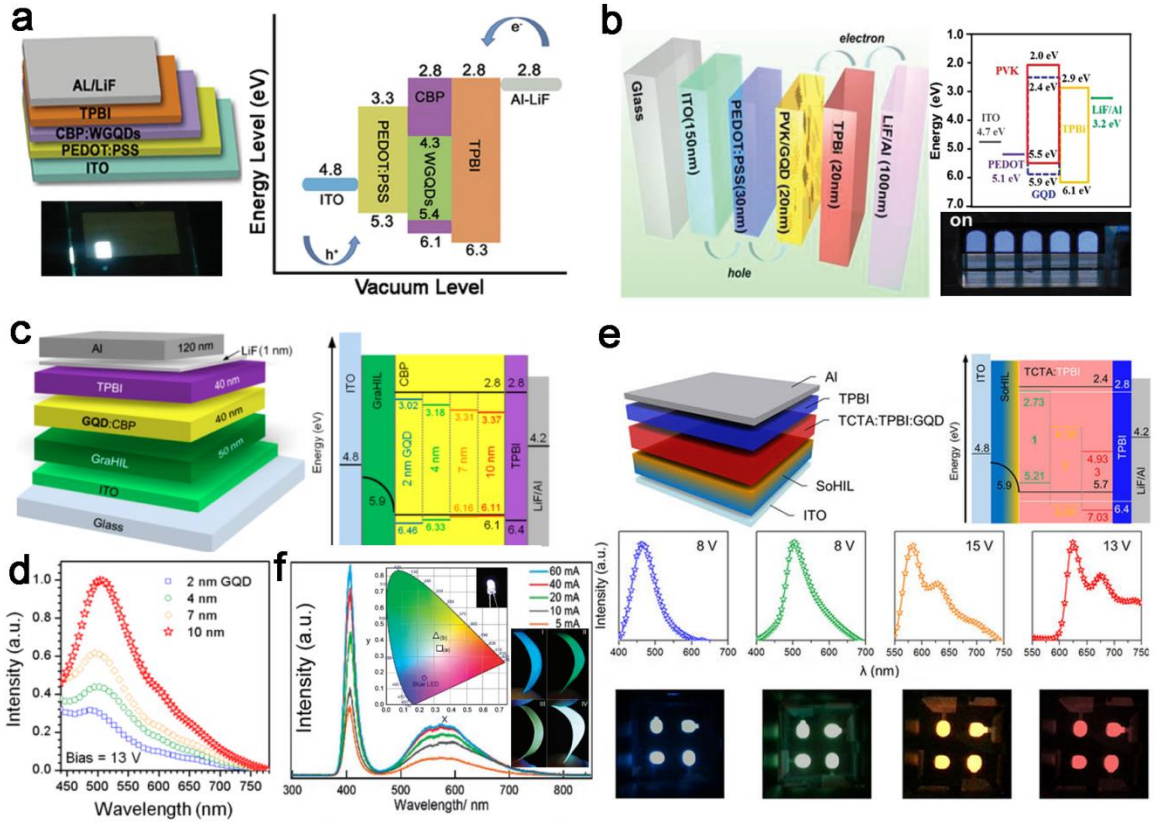

Figure 5 LED applications. (a) Physical and energy structure of a LED using GQDs as the electroluminescent phosphor,[8] permitted by John Wiley & Sons © 2016. (b) Structure of a LED using pristine GQDs as phosphor emitting blue light,[101] permitted by John Wiley and Sons © 2014. (c) Physical and electronic structures of an OLED using GQDs as light emitter, and (d) its electroluminescence spectra at bias 13 V,[38] permitted by American Chemical Society © 2014. (e) LED structure, energy levels, electroluminescence spectra, photographs of the blue, green, orange and red LEDs using aniline derivatives functionalized GQDs as bandgap tuner, permitted by Springer Nature © 2016.[37] (f) GQDs as color converter for LED,[104] permitted by Royal Society of Chemistry © 2015.

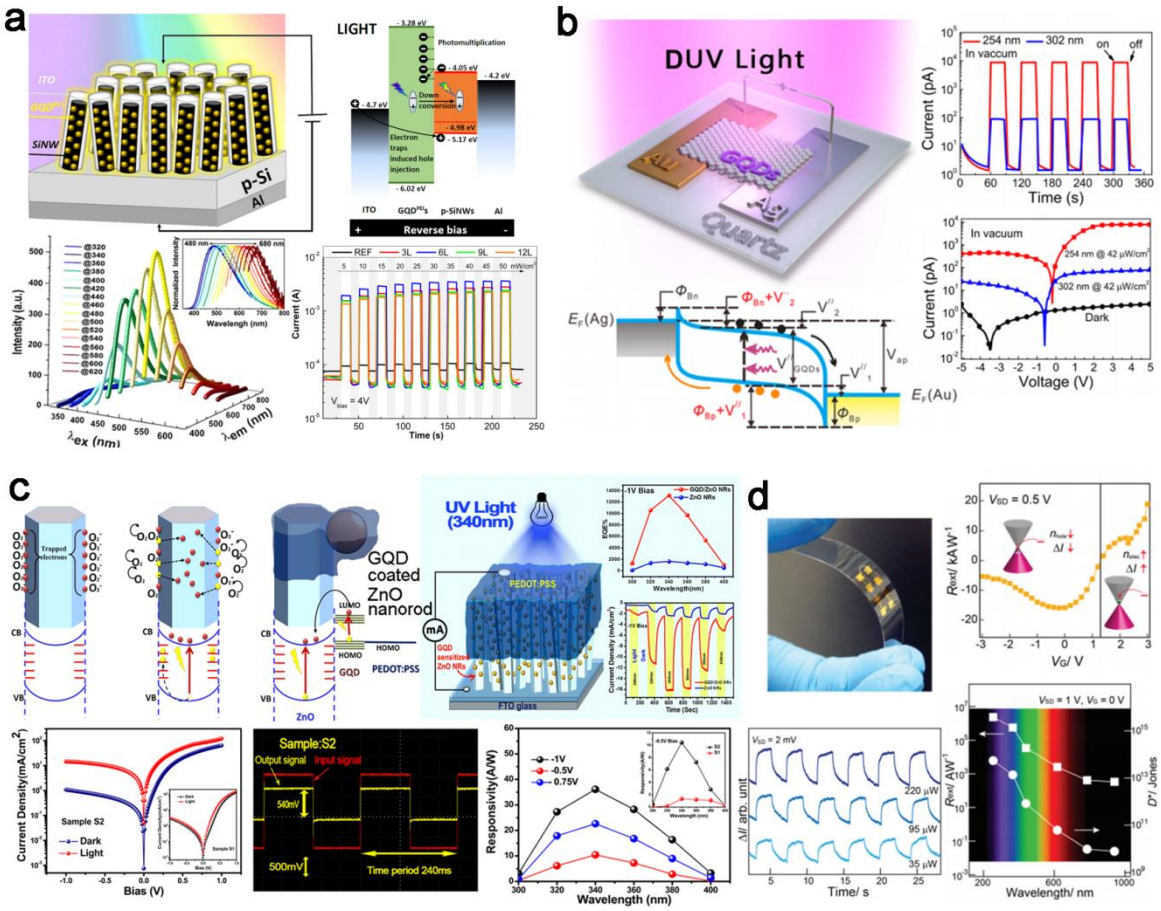

Figure 6 GQD-assisted photodetectors. (a) Photodetector based on GQD-sensitized Si nanowires,[105] permitted by American Chemical Society © 2017. (b) Deep UV photodetector uses large-bandgap GQDs,[107] permitted by American Chemical Society © 2015. (c) GQD/ZnO heterojunction as visible-blind UV photodetector,[109] permitted by American Chemical Society © 2016. (d) Red-emitted GQD/graphene/BN nanosheets are used as photodetector for broadband photodetection from UV to NIR,[111] permitted by Royal Society of Chemistry © 2016.

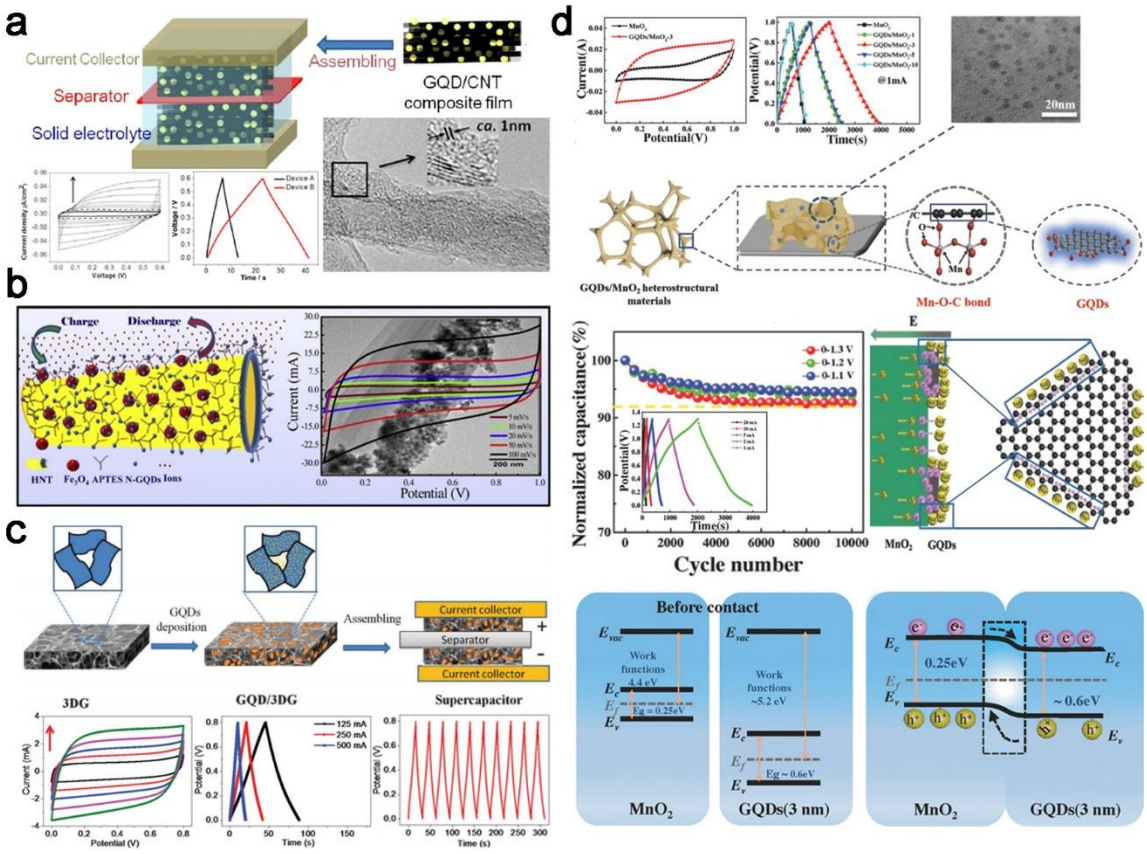

Figure 7 GQD-based supercapacitors. (a) A GQD/CNT hybrid supercapacitor,[115] permitted by IOP publishing © 2013. (b) GQD decorated Fe_3O_4-halloysite nanotubes as supercapacitor,[119] permitted by Elsevier © 2017. (c) GQD/3D graphene hybrid as supercapacitor,[123] permitted by Royal Society of Chemistry © 2014. (d) GQD/MnO_2 supercapacitor shows high potential window due to the built-in electric filed of the heterostructure region,[116] permitted by John Wiley & Sons © 2018.

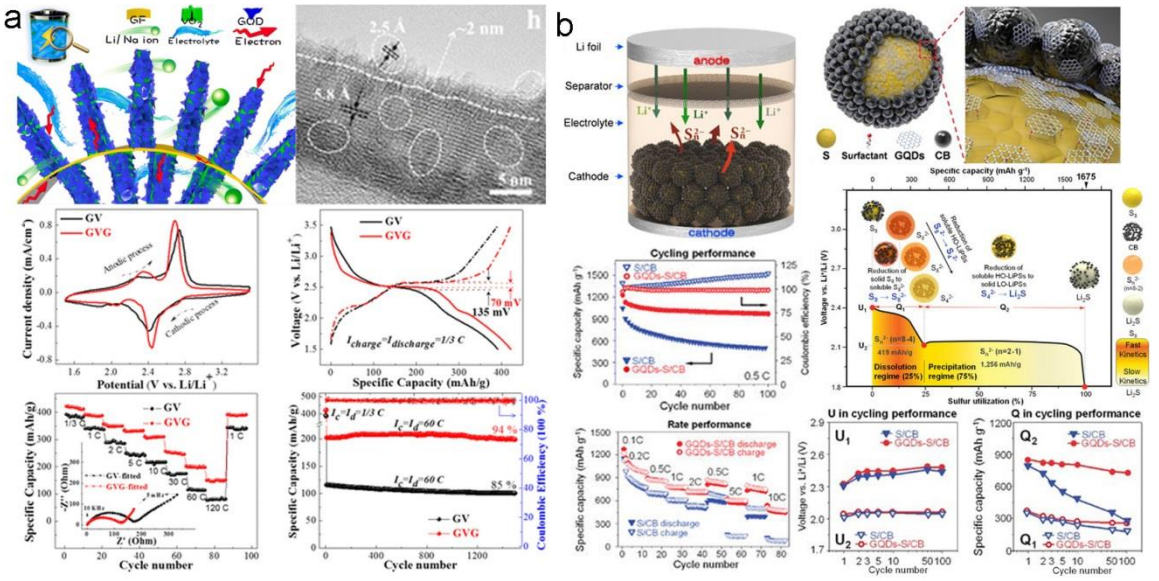

Figure 8 GQDs for batteries. (a) VO_2/graphene arrays coated with GQDs as the cathode for both Li-ion and Na-ion batteries,[131] permitted by American Chemical Society © 2015. (b) GQD-integrated sulfur-carbon as the cathode for Li-S battery,[128] permitted by Springer Nature © 2016.

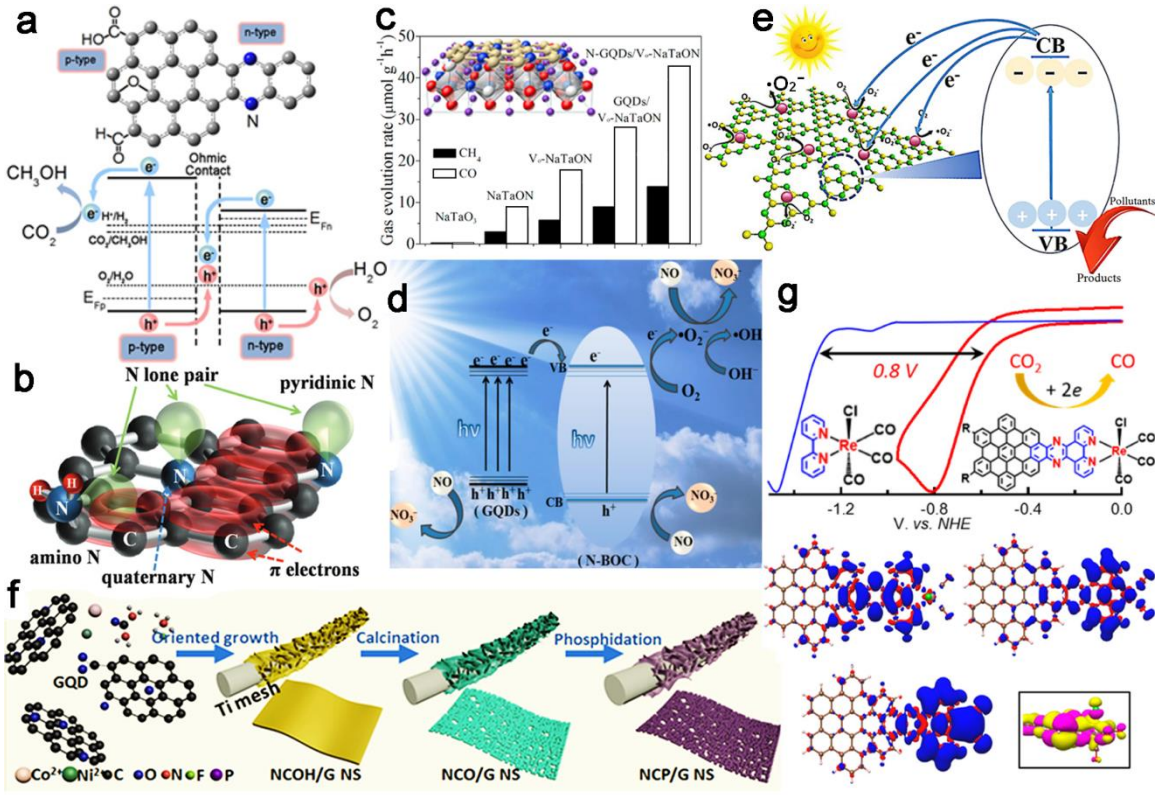

Figure 9 GQDs for catalysis applications. (a) GQD with intramolecular Z-scheme structure for photocatalysis, reprinted with permission by American Chemical Society © 2018.[86] (b) N-GQDs for hydrogen evolution,[25] permitted by John Wiley & Sons © 2016. (c) N-GQD/Vo-NaTaON for CO_2 reduction,[140] permitted by Elsevier © 2016. (d) GQD/N-$Bi_2O_2CO_3$ heterojunction for NO oxidation,[148] permitted by American Chemical Society © 2017. (e) GQD/C_3N_4 heterojunction for photocatalytic degradation of pollutant,[145] permitted by Elsevier Copyright 2017. (f) GQD engineered $NiCo_2P_2$ nanocatalyst for bifunctional overall water splitting,[5] permitted by Elsevier © 2018. (g) A GQD-Rhenium complex shows ultralow onset potential for CO_2 reduction into CO,[166] permitted by American Chemical Society © 2017.

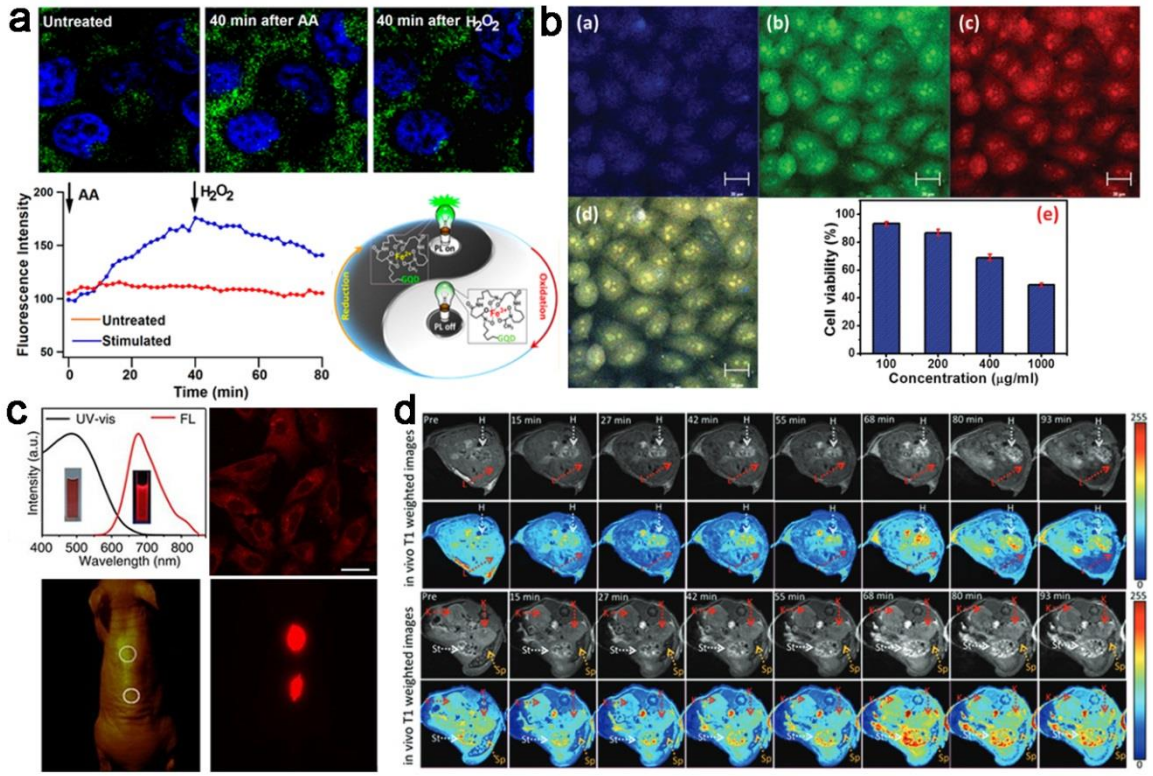

Figure 10 GQDs as the new class of fluorophores for bioimaging. (a) Using a GQD-DFOB-Fe^{3+}/Fe^{2+} probe to monitor the intracellular redox dynamics in real time,[181] permitted by American Chemical Society © 2016. (b) Confocal images of A549 cells labelled by S,N-GQDs under excitation of 405, 488, and 555 nm (scale bars 20 μm) and cell viability test,[138] permitted by John Wiley and Sons © 2015. (c) Red fluorescence (680 nm) emitting GQDs for cell imaging and in vivo imaging in mice,[72] permitted by Springer Nature © 2014. (d) MRI imaging of mice at different time duration after injection with B-doped GQDs (heart - H, liver - L, kidneys - K, spleen - Sp, and stomach - St),[80] permitted by John Wiley and Sons, copyright 2016.

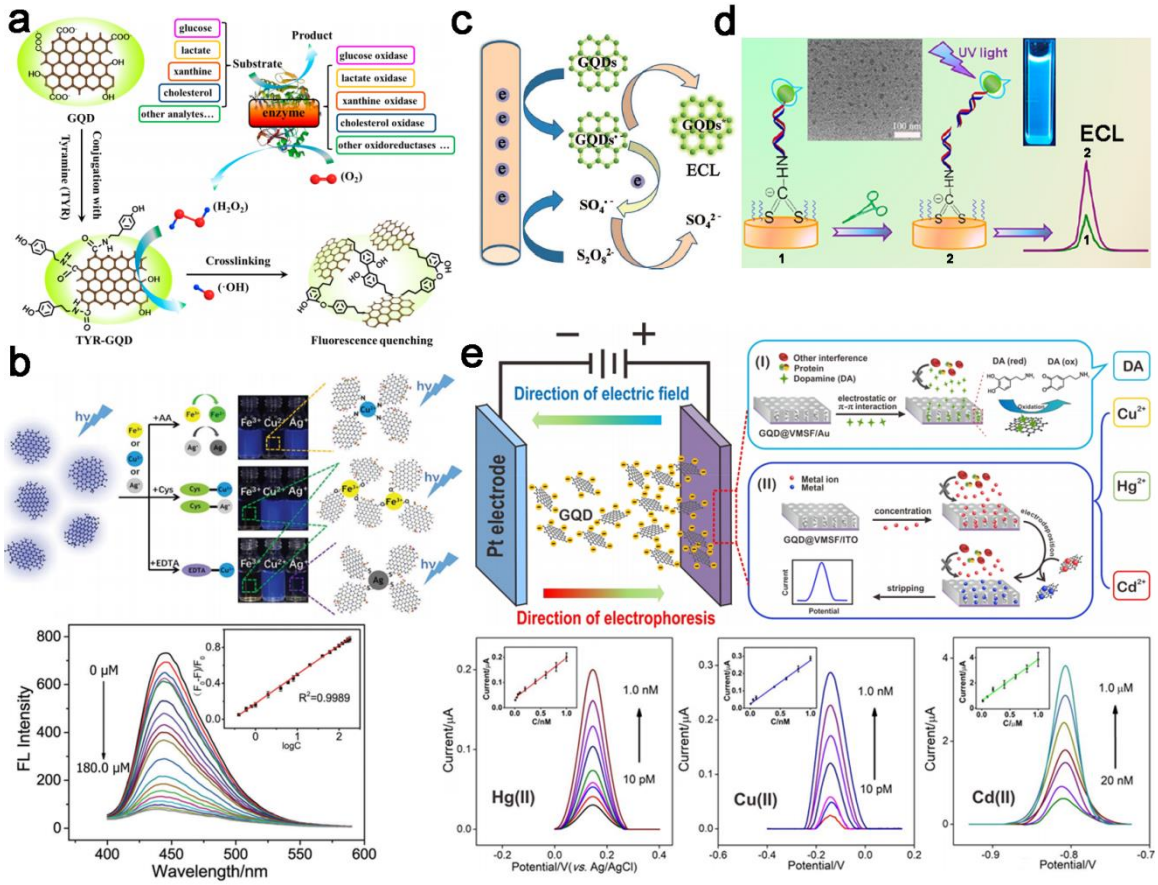

Figure 11 GQD based sensors. (a) PL sensing of metabolites using tyramine-functionalized GQDs,[189] permitted by American Chemical Society © 2016. (b) N,S-GQD based PL detection of metal ions,[15] permitted by Royal Society of Chemistry © 2017. (c) Illustration of cathodic ECL sensing using GQDs,[21] permitted by John Wiley and Sons. (d) ECL sensing of DNA strand,[200] permitted by American Chemical Society © 2015. (e) Ultrasenstive electrochemical detection of metal ions in complex samples using GQDs confined in the film of mesoporous silica-nanochannels,[205] permitted by American Chemical Society © 2018.

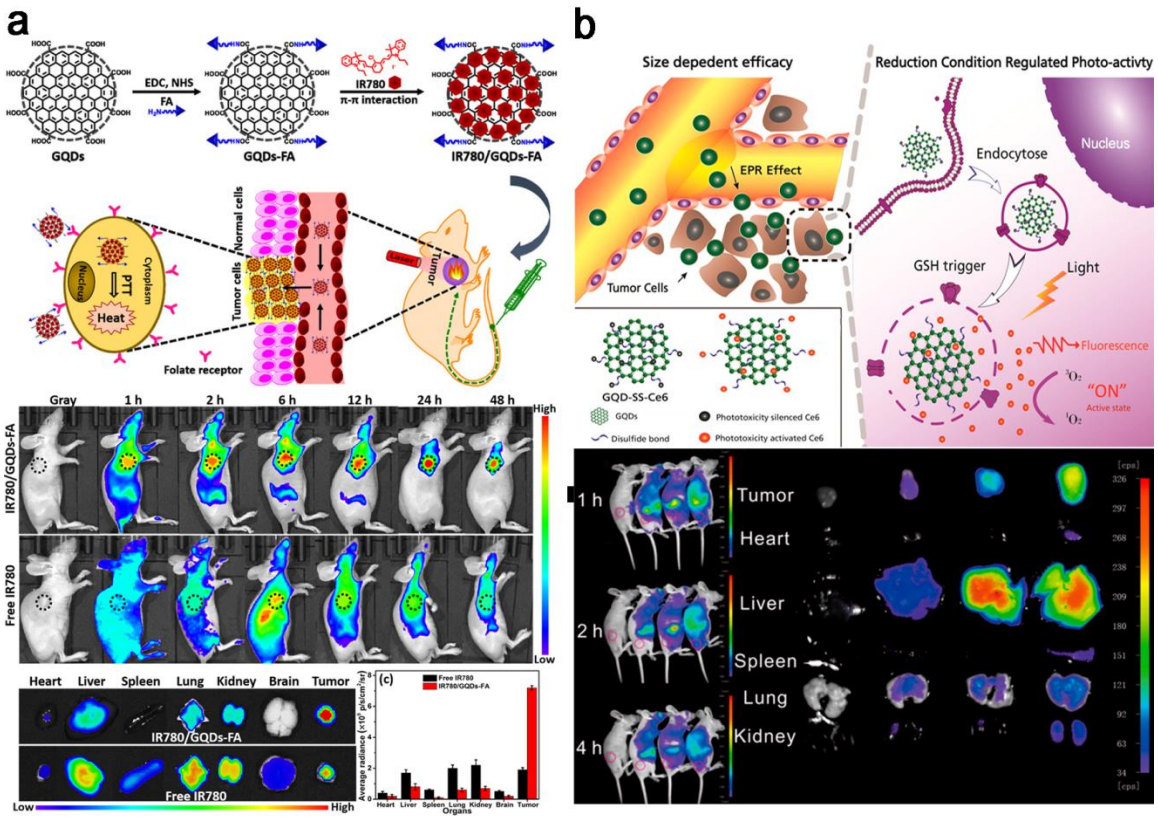

Figure 12 GQDs as the therapeutic agents. (a) Photothermal therapy using IR780/GQD functionalized with FA to kill cancer cells and eradicate tumor in mice,[218] permitted by American Chemical Society © 2017. (b) Photodynamic therapy using photosensitizer (chlorin e6) functionalized GQDs,[219] permitted by American Chemical Society, copyright 2016.